Available online at www.sciencedirect.com

ScienceDirect

Geochimica et Cosmochimica Acta 186 (2016) 71–90

Geochimica et Cosmochimica Acta

www.elsevier.com/locate/gca

# Fe hydroxyphosphate precipitation and Fe(II) oxidation kinetics upon aeration of Fe(II) and phosphate-containing synthetic and natural solutions

B. van der Grift [a,b,*], T. Behrends [c], L.A. Osté [b], P.P. Schot [a], M.J. Wassen [a], J. Griffioen [a,d]

[a] *Copernicus Institute of Sustainable Development, Faculty of Geosciences, Utrecht University, P.O. Box 80115, 3508 TA Utrecht, The Netherlands*

[b] *Deltares, P.O. Box 85467, 3508 AL Utrecht, The Netherlands*

[c] *Department of Earth Sciences, Faculty of Geosciences, Utrecht University, P.O. Box 80021, 3508 TA Utrecht, The Netherlands*

[d] *TNO Geological Survey of the Netherlands, P.O. Box, 80 015, 3508 TA Utrecht, The Netherlands*

Received 6 August 2015; accepted in revised form 19 April 2016; Available online 27 April 2016

**Abstract**

Exfiltration of anoxic Fe-rich groundwater into surface water and the concomitant oxidative precipitation of Fe are important processes controlling the transport of phosphate ($PO_4$) from agricultural areas to aquatic systems. Here, we explored the relationship between solution composition, reaction kinetics, and the characteristics of the produced Fe hydroxyphosphate precipitates in a series of aeration experiments with anoxic synthetic water and natural groundwater. A pH stat device was used to maintain constant pH and to record the $H^+$ production during Fe(II) oxidation in the aeration experiments in which the initial aqueous P/Fe ratios ($(P/Fe)_{ini}$), oxygen concentration and pH were varied. In general, Fe(II) oxidation proceeded slower in the presence of $PO_4$ but the decrease of the $PO_4$ concentration during Fe(II) oxidation due to the formation of Fe hydroxyphosphates caused additional deceleration of the reaction rate. The progress of the reaction could be described using a pseudo-second-order rate law with first-order dependencies on $PO_4$ and Fe(II) concentrations. After $PO_4$ depletion, the Fe(II) oxidation rates increased again and the kinetics followed a pseudo-first-order rate law. The first-order rate constants after $PO_4$ depletion, however, were lower compared to the Fe(II) oxidation in a $PO_4$-free solution. Hence, the initially formed Fe hydroxyphosphates also affect the kinetics of continuing Fe(II) oxidation after $PO_4$ depletion. Presence of aqueous $PO_4$ during oxidation of Fe(II) led to the formation of Fe hydroxyphosphates. The P/Fe ratios of the precipitates ($(P/Fe)_{ppt}$) and the recorded ratio of $H^+$ production over decrease in dissolved Fe(II) did not change detectably throughout the reaction despite a changing P/Fe ratio in the solution. When $(P/Fe)_{ini}$ was 0.9, precipitates with a $(P/Fe)_{ppt}$ ratio of about 0.6 were formed. In experiments with $(P/Fe)_{ini}$ ratios below 0.6, the $(P/Fe)_{ppt}$ decreased with decreasing $(P/Fe)_{ini}$ and pH value. Aeration experiments with natural groundwater showed no principal differences in Fe(II) oxidation kinetics and in $PO_4$ immobilisation dynamics compared with synthetic solutions with corresponding P/Fe ratio, pH and oxygen pressure. However, aeration of groundwater with relative high DOC concentrations and a low salinity lead to P-rich Fe colloids that were colloidally stable. The formation of a Fe hydroxyphosphate phase with a molar P/Fe ratio of 0.6 can be used for predictive modelling of $PO_4$ immobilisation upon aeration of pH-neutral natural groundwater with an $(P/Fe)_{ini}$ ratio up to 1.5. These findings provide a solid basis for further studies on transport and bioavailability of phosphorus in streams, ditches and channels that receive anoxic Fe-rich groundwater.



* Corresponding author at: Deltares, P.O. Box 85467, 3508 AL Utrecht, The Netherlands. Tel.: +31 623478769.
*E-mail address:* bas.vandergrift@deltares.nl (B. van der Grift).

http://dx.doi.org/10.1016/j.gca.2016.04.035
0016-7037/

*Keywords:* Iron; Kinetics; Oxidation; Phosphate; Precipitation (chemistry); Redox conditions; Groundwater; Aeration; Colloids; Fe hydroxyphosphates; Aqueous solution

## 1. INTRODUCTION

The chemistry of phosphate in aquatic systems is often controlled through interactions with iron (Fox, 1989; Mayer and Jarrell, 2000). Under oxidising conditions, aqueous phosphate has a strong affinity to associate with Fe oxyhydroxides (Filippelli, 2008). Association with Fe oxyhydroxides may include adsorption, surface precipitation, formation of solid solutions and co-precipitation (van Riemsdijk et al., 1984; Fox, 1989; Dzombak and Morel, 1990; Ler and Stanforth, 2003; Griffioen, 2006; Voegelin et al., 2010). Iron associated $PO_4$ can be solubilised under reducing conditions due to reductive dissolution of Fe oxyhydroxides (Mayer and Jarrell, 2000). However, under anoxic conditions, mobilisation of $PO_4$ can be limited due to formation of Fe(II)-phosphate minerals such as vivianite (Roden and Edmonds, 1997; Heiberg et al., 2012). Redox transformations of iron in natural environments thus exert a strong influence on the mobility of $PO_4$.

Lowland areas, like the Netherlands, typically have redox-reactive aquifers containing anoxic Fe(II)-rich groundwater (Frapporti et al., 1993; Griffioen et al., 2013). When Fe(II)-rich groundwater enters surface water, Fe(III) precipitates are formed at the groundwater-surface water interface upon oxygenation of the anoxic groundwater (Vanlierde et al., 2007; Baken et al., 2013, 2015b; van der Grift et al., 2014). The formation of Fe oxyhydroxides during groundwater exfiltration is expected to be accompanied by the immobilisation of aqueous phosphate due to its association with the Fe precipitates (Griffioen, 1994; Baken et al., 2015a). The release of $PO_4$ to surface water following $PO_4$ leaching from heavily fertilised agricultural fields to groundwater and the extent of $PO_4$ retention at the redox interface are of major importance for surface water quality (Schoumans and Chardon, 2014; Baken et al., 2015b). Based on field data, Van der Grift et al. (2014) proposed that the formation of Fe(III) phosphate precipitates can be an important natural immobilisation mechanism for aqueous $PO_4$ during flow of groundwater into surface water. This may reduce the $PO_4$ load from agricultural land to surface water. Consequently, formation of Fe(III) phosphates at redox interfaces might be a major control on the $PO_4$ transport in the continuum from land to sea and on the bioavailability of $PO_4$ in natural waters that drain anoxic aquifers. Detailed insight into the chemical stoichiometry and the kinetics of formation of Fe(III) phosphate phases during oxygenation of anoxic, Fe and $PO_4$ containing groundwater is therefore of great interest.

Precipitation of Fe(III) from $PO_4$ containing aqueous solutions is expected to lead to the formation of Fe hydroxyphosphates (Stumm and Morgan, 1970) with variable P/Fe ratio according to the stoichiometry:

$$r\mathrm{Fe}^{3+} + \mathrm{PO}_4^{3-} + (3r-3)\mathrm{OH}^- \rightarrow \mathrm{Fe}_r\mathrm{PO}_4(\mathrm{OH})_{3r-3}(\mathrm{s}) \quad (1)$$

where $1/r$ is the stoichiometric molar P/Fe ratio of the Fe hydroxyphosphate. The solubility constants for mineral phases have been reported for $r = 1$ (strengite) by Nriagu (1972) and later by Iuliano et al. (2007), for $1/r = 0.66$ (tinticite) by Nriagu and Dell (1974) and for $1/r = 0.4$ by Luedecke et al. (1989). Pratesi et al. (2003) described the existence of an amorphous Fe hydroxyphosphate, santabarbaraite, with a $1/r$ value of 0.66 but no solubility data were presented. Iron(III) phases with high P/Fe ratios have been identified in natural systems such as lakes (Buffle et al., 1989; Lienemann et al., 1999; Gunnars et al., 2002) as well as estuarine or lake sediments (Tessenow, 1974; Hyacinthe and Van Cappellen, 2004). Precipitation of these phases has also been reported as a mechanism for $PO_4$ removal from wastewater (Stumm and Sigg, 1979; Luedecke et al., 1989; Fytianos et al., 1998).

Formation of Fe hydroxyphosphates induced by Fe(II) oxidation at near-neutral pH has been investigated in various studies (Einsele, 1934; Tessenow, 1974; Lienemann et al., 1999; Mayer and Jarrell, 2000; Matthiesen et al., 2001; Gunnars et al., 2002; Griffioen, 2006; Kaegi et al., 2010; Voegelin et al., 2010, 2013; Senn et al., 2015). Phosphate uptake per oxidised Fe was found to be limited to a P/Fe molar ratio of ≈0.5–0.6 under varying experimental conditions regarding initial Fe(II) and $PO_4$ concentrations, pH and background electrolytes, (Tessenow, 1974; He et al., 1996; Gunnars et al., 2002; Voegelin et al., 2013). This suggests the formation of a single type of Fe hydroxyphosphate phase at initial aqueous P/Fe ($(P/Fe)_{ini}$) ratios larger than ≈0.5. A limited number of studies indicate that P-rich precipitates with molar P/Fe ratio of 0.5–0.6 can form in the beginning of Fe(II) oxidation even when the $(P/Fe)_{ini}$ is less than 0.5 (Einsele, 1934; Tessenow, 1974; Deng, 1997; Gunnars et al., 2002; Voegelin et al., 2013). As a consequence, the P/Fe ratio in the solution progressively decreases when precipitates form which are relatively enriched in P. By using TEM and XAS, Voegelin et al. (2013) showed that, in solutions with $(P/Fe)_{ini}$ less than 0.5, early formation of amorphous Fe hydroxyphosphates is followed by the formation of short-range ordered ferrihydrite-type precipitates in silicate-containing solutions or poorly-crystalline lepidocrocite in silicate-free solutions when the solution becomes depleted in $PO_4$. The sequential precipitation of Fe hydroxyphosphates followed by precipitation of Fe oxyhydroxides during Fe(II) oxidation indicates that formation of Fe hydroxyphosphates with a P/Fe ratio around 0.5–0.6 is either kinetically controlled or Fe hydroxyphosphates with a P/Fe ratio around 0.5–0.6 are the thermodynamically favoured precipitates in the initial stage of homogeneous nucleation due to low surface energies (Navrotsky et al., 2008). The molar P/Fe ratio in precipitates was also around 0.5–0.6 in studies on As removal in presence of $PO_4$. This finding has been used to rationalize variations in the efficiency of As removal techniques from drinking water in areas with different groundwater chemistry (Roberts et al., 2004; Hug et al., 2008). Since the P/Fe ratios in the Fe hydroxyphosphates seem to vary to a small extent for several experimental

conditions, it is likely that these precipitates cannot be considered as a distinct mineral phase. Several authors observed, for instance, that Fe-$PO_4$ solids in natural systems contain other major cations like Ca (Perret et al., 2000; Matthiesen et al., 2001). Senn et al. (2015) recently published results of Fe(II) aeration experiments in $PO_4$ and Ca containing solutions and showed that the formed precipitates are not distinct phases but mixtures of different types of polymers whose fractional contribution gradually varies with solution chemistry. In addition, Voegelin et al. (2013) measured P/Fe ratios in precipitates that formed at different time intervals during Fe(II) oxidation. The P/Fe ratios varied in a single experiment indicating that not a distinct Fe-$PO_4$ phase is formed but that the precipitates are a solid-solution whose composition depends on the $PO_4$ activities in the solution. Fox (1989) argued that $PO_4$ levels in rivers with low calcium concentrations are controlled by a solid-solution of Fe phosphate and Fe oxyhydroxide.

The kinetics of Fe(II) oxidation and precipitation of Fe oxyhydroxides has been investigated intensively (e.g. Stumm and Lee, 1961; Sung and Morgan, 1980; Davison and Seed, 1983; Millero, 1985), but there is a limited number of studies that addressed the kinetics of Fe(II) oxidation in presence of $PO_4$ (Tamura et al., 1976; Mitra and Matthews, 1985; Cumplido et al., 2000; Wolthoorn et al., 2004; Mao et al., 2011). These studies indicate that the presence of $PO_4$ affects the kinetics of Fe(II) oxidation. Phosphate accelerates the oxidation of dissolved Fe(II) (Tamura et al., 1976; Mitra and Matthews, 1985; Mao et al., 2011). Tamura et al. (1976) found that the rate of oxidation of micromolar Fe(II) could be expressed as a function of the concentration of $H_2PO_4^-$. Conversely, Mitra and Matthews (1985) concluded that $HPO_4^{2-}$ was the sole phosphate species controlling the Fe(II) oxidation rate. Mao et al. (2011) found that the aqueous phosphate complex $FePO_4^-$ was the most important Fe(II) species contributing to the oxidation kinetics of nanomolar Fe(II) at circumneutral pH. Cumplido et al. (2000) showed that the rate of Fe(II) oxidation in presence of Fe oxyhydroxides phases accelerates with increasing $PO_4$ concentrations. Oxidation of adsorbed Fe(II) slows down in heterogeneous systems upon addition of $PO_4$ as shown by Wolthoorn et al. (2004). None of these studies characterised the kinetics of Fe(II) oxidation when the composition of the Fe(III)-precipitates changes during the reaction. This is usually the case when Fe(II) containing groundwater becomes exposed to atmospheric oxygen because the initial P/Fe ratio is typically below 0.5.

Most experimental work on $PO_4$ immobilisation induced by Fe(II) oxidation have used synthetic solutions. However, the presence of other constituents in natural groundwater can additionally alter the Fe(II) oxidation kinetics and $PO_4$ immobilisation. Studies that use natural groundwater are, to our knowledge, limited to the work of Baken et al. (2013) and Griffioen (2006) and the applicability of experimental results on $PO_4$ immobilisation during groundwater seepage into surface water is still unclear. For example, Griffioen (2006) was not able to model the immobilisation of $PO_4$ by Fe oxide type phases that form upon oxygenation of dissolved Fe(II) in natural groundwater using existing solid phase association concepts.

In this study we aim to: (1) determine the P/Fe ratios in Fe hydroxyphosphates that form during Fe(II) oxidation in presence of $PO_4$ as a function of pH, the initial aqueous P/Fe ratio and the reaction progress; (2) establish the kinetics of Fe(II) oxidation upon aeration of synthetic solutions with varying P/Fe ratios; (3) assess the effectiveness of the formation of Fe-$PO_4$ phases to immobilise $PO_4$ when natural Fe(II) and $PO_4$-containing groundwater is exposed to atmospheric oxygen; and (4) explore the possibility of using predictive mechanistic models for $PO_4$ immobilisation during groundwater seepage. Oxidation of Fe(II) was studied in a series of time-resolved aeration experiments with synthetic water and natural groundwater with variable $(P/Fe)_{ini}$ while pH values and oxygen concentrations were kept constant at various levels. The combination of continuously monitoring acid production with a pH stat device and discrete sampling and analyses allowed us to follow the kinetics of the reaction and the chemical composition of the precipitates throughout the experiments.

## 2. MATERIALS AND METHODS

### 2.1. Batch experiments with synthetic solutions

Aeration experiments with synthetic aqueous solutions were carried out at Fe(II) concentrations between 0.2 and 0.27 mmol $L^{-1}$ and $PO_4$ concentrations in the range of 0–0.18 mmol $L^{-1}$. Hence, initial aqueous P/Fe ratios ($(P/Fe)_{ini}$) were varied between 0 and ≈0.9 (Table 1). The experimental setup was similar to that used by Vollrath et al. (2012). The experiments were carried out in a 1 litre glass reactor with an electrically powered stirrer (Applikon Stirrer Controller P100) and a dissolved oxygen sensor (Applisens DO2 sensor, low drift). The drift of the sensor is negligible and the response time is less than 30 seconds. The pH was kept constant during the experiment using an automated pH stat device which delivered a 0.01 mol $L^{-1}$ NaOH solution to the reactor vessel (Metrohm unitrode PT 100 electrode coupled to titrino Metrohm 736 GP controlled by TiNET 2.4 software). The oxygen concentration was kept constant during the experiments by purging a gas with defined $O_2$ content through the reactor. The $O_2$ content of the gas was maintained by a mass flow control unit (Bronkhorst HI-TEC) that regulated gas mixtures of compressed air and argon. In the experiments with synthetic solutions, the gas was conveyed through two gas washing bottles, first through a bottle with soda lime pellets followed by a bottle with a 0.05 mol $L^{-1}$ NaOH solution in order to remove $CO_2$. Then the gas was humidified in a third gas-washing bottle before it finally entered the reactor. The experiments with synthetic solutions were performed using 500 ml 4.8 mmol $L^{-1}$ KCl background electrolyte solution. The stirring rate was set to 200 rpm to minimise local pH fluctuations during NaOH addition. A solution of 0.2 mol $L^{-1}$ $Fe(NH_4)_2(SO_4)_2{\cdot}6H_2O$ in 0.032 mol $L^{-1}$ HCl was used as Fe(II) stock. The stock solution was kept constantly under Ar atmosphere in a glovebox to prevent iron oxidation. A solution of

Table 1
Overview of synthetic solutions aeration experiments. The experimental stages before and after near-depletion of $PO_4$ are indicated as $PO_4$ stage and $PO_4$ free stage, respectively.

| P/Fe ratio initial | pH | $O_2$ mg $L^{-1}$ | P/Fe ratio precipitates[a] | Stoichiometry precipitate | $(H^+/Fe^{2+})$ ratio measured $PO_4$ stage | $(H^+/Fe^{2+})$ ratio PHREEQC $PO_4$ stage | $(H^+/Fe^{2+})$ ratio measured $PO_4$ free stage | $t_{3/4}$[b] min | Fe(II) normalised oxidation rate $PO_4$ stage $min^{-1}$ | First-order rate constant $PO_4$ free stage $min^{-1}$ | Second-order rate constant $PO_4$ stage $\mu mol^{-1}$ L $min^{-1}$ | Moment $PO_4$ depletion min | Moment $dFe/dt$ minimal min |
|---|---|---|---|---|---|---|---|---|---|---|---|---|---|
| 0 | 6.1 | 8.5 | 0 | $Fe(OH)_3$ | – | – | 1.94 | 390 | – | 0.0039 | – | – | – |
| 0 | 6.1 | 10.5 | 0 | $Fe(OH)_3$ | – | – | 1.93 | 290 | – | 0.0049 | – | – | – |
| 0 | 6.4 | 3.5 | 0 | $Fe(OH)_3$ | – | – | 1.90 | 300 | – | 0.0053 | – | – | – |
| 0.90 | 6.1 | 8.5 | $0.60 \pm 0.01$ | $Fe_{1.67}PO_4(OH)_{2.01}$ | 1.33 | 1.31 | – | 790 | 0.0022–0.0011 | – | $1.53 \times 10^{-5}$ | – | – |
| 0.93 | 6.1 | 10.5 | $0.61 \pm 0.01$ | $Fe_{1.64}PO_4(OH)_{1.92}$ | 1.33 | 1.30 | – | 460 | 0.0034–0.0018 | – | $2.78 \times 10^{-5}$ | – | – |
| 0.93 | 6.1 | 10.5 | $0.61 \pm 0.01$ | $Fe_{1.64}PO_4(OH)_{1.92}$ | 1.33 | 1.30 | – | 480 | 0.0032–0.0016 | – | $2.48 \times 10^{-5}$ | – | – |
| 0.96 | 6.4 | 3.6 | $0.56 \pm 0.01$ | $Fe_{1.79}PO_4(OH)_{2.37}$ | 1.27 | 1.29 | – | 750 | 0.0023–0.0014 | – | $1.79 \times 10^{-5}$ | – | – |
| 0.30 | 6.1 | 10.5 | $0.48 \pm 0.02$ | $Fe_{2.08}PO_4(OH)_{3.24}$ | 1.42 | 1.46 | 1.95 | 2020 | 0.003–0.0003 | 0.0007 | $5.25 \times 10^{-5}$ | 790 | 1180 |
| 0.28 | 6.4 | 3.6 | $0.44 \pm 0.02$ | $Fe_{2.27}PO_4(OH)_{3.81}$ | 1.47 | 1.47 | 1.85 | 1670 | 0.0013–0.0004 | 0.0013 | $3.53 \times 10^{-5}$ | 1000 | 1460 |
| 0.18 | 6.1 | 10.5 | $0.41 \pm 0.02$ | $Fe_{2.44}PO_4(OH)_{4.32}$ | 1.55 | 1.52 | 1.89 | 1890 | 0.003–0.0004 | 0.0008 | $1.13 \times 10^{-4}$ | 480 | 760 |
| 0.18 | 6.4 | 3.6 | $0.36 \pm 0.02$ | $Fe_{2.78}PO_4(OH)_{4.34}$ | 1.48 | 1.54 | 1.91 | 930 | 0.004–0.0007 | 0.0022 | $9.46 \times 10^{-5}$ | 430 | 490 |
| 0.12 | 6.1 | 10.5 | $0.39 \pm 0.01$ | $Fe_{2.56}PO_4(OH)_{4.68}$ | 1.48 | 1.54 | 1.85 | 1200 | 0.0015–0.0005 | 0.0014 | $5.72 \times 10^{-5}$ | 340 | 390 |
| 0.12 | 6.4 | 3.6 | $0.40 \pm 0.02$ | $Fe_{2.5}PO_4(OH)_{4.5}$ | 1.46 | 1.49 | 1.84 | 890 | 0.0001–0.0007 | 0.0023 | $4.08 \times 10^{-5}$ | 380 | 430 |

[a] Average value and standard deviation of series of calculated $(P/Fe)_{ppt}$ ratio bases on the decrease in measured Fe(II) and $PO_4$ concentrations.
[b] Time required for 75% Fe(II) oxidation.

0.2 mol $L^{-1}$ $KH_2PO_4$ was used as $PO_4$ stock. The KCl solution was purged with Ar prior to Fe(II) addition until the concentration of $O_2$ in solution concentration was lower than 0.001 mmol $L^{-1}$. Next, the reactor was spiked with the desired amount of the $PO_4$ stock solution and Fe(II) stock solution. The Fe(II) oxidation experiment was started by switching from Ar to pressurised air or a pressurised air/Ar mixture in the purging gas. The desired $O_2$ level was reached in the reactor within a few minutes after changing the gas composition. The experiments were conducted in a climate controlled room at 20 °C.

*2.1.1. Monitoring reaction progress*

The reaction progress was followed by continuously monitoring the supply of NaOH by the pH stat device. Before and during the experiment, samples were taken from the solution in the reactor to follow the evolution of Fe(II), Fe(III) and $PO_4$ concentrations over time. Each sample (6 ml) was retrieved with a syringe from the reactor and was immediately filtered through 0.45 μm nylon membranes and acidified to a pH = 1.5 using a 6 M HCl solution. The Fe(II) concentrations were measured within 6 h after sampling. The concentrations were determined using spectrophotometric methods. Iron(II) and total-Fe were measured in separate sub-samples using the ferrozine method from Viollier et al. (2000). In the total-Fe subsample, Fe(III) was reduced to Fe(II) using a hydroxylamine hydrochloride solution. The Fe(II) concentrations were measured spectrophotometrically with ferrozine at 562 nm (Shimadzu UV Spectrophotometer, UV-1800) against standard series in a range between 0 and 100 μmol $L^{-1}$ obtained with $Fe(NH_4)_2(SO_4)_2{\cdot}6H_2O$ (Sigma-Aldrich) in 0.5 mol $L^{-1}$ HCl. The Fe(III) concentrations were calculated from the differences between total-Fe and Fe(II) concentrations. The detection limit of the spectrophotometric method was 3 μmol $L^{-1}$. The 95% confidence interval of the calibration line varied between 1.2 and 2.3 μmol $L^{-1}$, leading to an uncertainty of the measured concentration that ranged between 55% at the detection limit and 1.4% in the middle of the calibration range.

Phosphate concentrations were determined according to the molybdenum blue method of Koroleff (1983). This method is based on the reaction of the $PO_4$ ion with an acidified molybdate reagent to yield a phosphomolybdate complex, which is then reduced to the intensely coloured mixed-valence complex. The $PO_4$ concentrations were measured at 880 nm against standard series in a range between 0 and 25 μmol $L^{-1}$ prepared with $KH_2PO_4$ (Fulka-analytical). The detection limit of the spectrophotometric method was 1 μmol $L^{-1}$. The 95% confidence interval of the calibration line varied between 0.14 and 0.17 μmol $L^{-1}$, leading to an uncertainty of the measured concentrations that ranged between 15% at the detection limit and 0.4% for concentrations in the middle of the calibration range.

The Fe/P ratio in the precipitates ($(Fe/P)_{ppt}$) was calculated from the reduction of dissolved Fe(II) and $PO_4$ concentrations over the duration of the experiment. The Fe(III) concentrations during the oxidation reaction were in a range from −6 to 9 μmol $L^{-1}$ (details in the supplementary material, Fig. S1) and were in the range of the uncertainties related to the different measurement. This indicated that colloidal Fe(III) was effectively retained by the filter membranes and that Fe passing the filter was mostly dissolved Fe(II).

*2.1.2. Reaction stoichiometry*

According to the ideal stoichiometry of Fe(II) oxidation by oxygen followed by precipitation of Fe hydroxide, 2 moles of protons are released per mole oxidised Fe(II):

$$Fe^{2+} + 0.25O_2 + 2.5H_2O \rightarrow \ Fe(OH)_3 + 2H^+ \quad (2)$$

Incorporation of water molecules or anions other than hydroxide in freshly formed Fe oxyhydroxides results in stoichiometric ratios between $H^+$ production and Fe(II) oxidation lower than 2 (Fox, 1988; Bonneville et al., 2004; Vollrath et al., 2012). Hence, the stoichiometric ratio between produced $H^+$ and oxidised Fe(II) is expected to be lower when Fe hydroxyphosphates form during Fe(II) oxidation compared to formation of pure Fe oxyhydroxides. For a Fe hydroxyphosphate with the general empirical stoichiometry $Fe_rPO_4(OH)_{3r-3}(s)$ the molar P/Fe ratio of the precipitates equals $1/r$ (Eq. (1)). In solutions with $H_2PO_4^-$ as the sole aqueous phosphate species, $2 - 1/r$ moles of protons are released per mole $Fe^{2+}$ oxidised:

$$rFe^{2+} + 1/4rO_2 + H_2PO_4^- + (2.5r - 3)H_2O \rightarrow Fe_rPO_4(OH)_{3r-3(s)} + (2r - 1)H^+ \quad (3)$$

An increase in the molar P/Fe ratio of the precipitate results in a decrease of the amount of produced protons per oxidised aqueous Fe(II) (hereinafter referred to as the molar $H^+/Fe^{2+}$ ratio) with a lowest possible $H^+/Fe^{2+}$ ratio of 1 for $r = 1$, resembling the precipitation of strengite ($FePO_4{\cdot}2H_2O$). The speciation of the phosphoric acid depends on pH and changes in the phosphoric acid speciation have an impact on the $H^+/Fe^{2+}$ ratio. Geochemical modelling was used to calculate the effect of phosphoric acid speciation on the $H^+/Fe^{2+}$ ratio (see Section 2.1.3).

For each experiment, the molar $H^+/Fe^{2+}$ ratio was calculated from the Fe(II) concentration measured directly on the discrete samples and the continuously recorded NaOH consumption. The experimentally derived molar $H^+/Fe^{2+}$ ratio can be used to derive the $(P/Fe)_{ppt}$ of the Fe hydroxyphosphates by geochemical modelling based on Eq. (3). By this, we evaluated whether the derived $H^+/Fe^{2+}$ ratio for one experiment with Fe hydroxyphosphate formation is consistent with the measured $(P/Fe)_{ppt}$ ratios obtained from the loss of dissolved Fe(II) and $PO_4$ which was measured in discrete samples.

The $H^+/Fe^{2+}$ calculation ignores Fe(II) associated with the particulate phase. It is not unlikely that Fe(II) oxidation triggers precipitation of an initially mixed-valence Fe(II, III) hydroxyphosphate. Under corresponding conditions, initial uptake of Fe(II) by Fe hydroxyphosphates has been documented by Voegelin et al. (2013). Replacement of Fe(III) by Fe(II) does not change the number of released $H^+$ at a given $(P/Fe)_{ppt}$ ratio (details in the supplementary material). That is, solid phase Fe(II) oxidation without a change in the $(P/Fe)_{ppt}$ does not result in further $H^+$ production or consumption. Iron(II) association with the solid phase has, thus, no effect on the interpretation of $(P/Fe)_{ppt}$

ratios based on the measured $H^+$ production over dissolved Fe(II) decrease. Iron(II) association with the particulate phase can also be caused by surface complexation of Fe (II) on ferrihydrite. Surface complexation modelling calculations indicated that the fraction adsorbed Fe(II) is less 0.5% during the initial state of the reaction and can be, hence, neglected.

The continuous evolution of dissolved Fe(II) concentration with time was obtained from the continuously monitored NaOH addition and the molar $H^+/Fe^{2+}$ ratio. The continuous evolution of Fe(II) concentration was used to explore the Fe(II) oxidation kinetics throughout the experiments. Since Fe(II) association with the particulate phase is ignored, the Fe(II) oxidation rates can be considered as maximum values.

#### 2.1.3. Geochemical modelling

PHREEQC (Parkhurst and Appelo, 1999) with the WATEQ4F database (Ball and Nordstrom, 1991) was used for modelling the $H^+/Fe^{2+}$ molar ratio according to Eq.(3) for the experiments with synthetic solutions and for predictive modelling for $PO_4$ immobilisation during groundwater seepage. Therefore, data were used from groundwater aeration experiments published by Griffioen (2006). In this study, fast immobilisation of $PO_4$ (<1 day) was investigated in aeration experiments with nutrient-rich anoxic groundwater having a wide variety in chemical composition and $(P/Fe)_{ini}$ ratios ranging from 0.07 to 40. The synthetic solution experiments were geochemically modelled starting with the measured initial Fe(II) and $PO_4$ concentrations, pH, temperature and the concentration of the background electrolyte. The groundwater experiments from Griffioen (2006) were modelled starting with the measured groundwater composition. Next, a constant oxygen pressure was imposed ($P_{O_2} = 0.2$ atm) and, by this, the equilibrium Fe redox state changed and Fe(II) became oxidised to Fe (III). The activities of the various species in solution, the precipitation of the Fe hydroxyphosphate, the molar $H^+/Fe^{2+}$ ratio (Eq. (3)) and the residual $PO_4$ concentrations after precipitation of Fe hydroxyphosphates were calculated with PHREEQC. For describing the precipitation of Fe hydroxyphosphates $Fe_rPO_4(OH)_{3r-3(s)}$ we used the solubility constant of $Fe_{2.5}PO_4(OH)_{4.5}$ (Luedecke et al., 1989) with a $r$ value of 2.5:

$$Log\ K_{Fe_{2.5}PO_4(OH)_{4.5}} = 2.5\ log[Fe^{3+}] + log[PO_4^{3-}] + 4.5\ log[OH^-] = -96.7 \quad (4)$$

wherein [i] refers to the activity of species i. Solubility constants for Fe hydroxyphosphates with $r$ values deviating from 2.5 were calculated from Eq. (4) using PHREEQC and the assumption that the solubility of the Fe hydroxyphosphates did not change significantly within the range of $r$ values of our experiments. Therefore, we replaced the stoichiometric coefficients in Eq. (4) with the corresponding values and calculated the *Ion Activity Product* (*IAP*) for the Fe hydroxyphosphate $Fe_rPO_4(OH)_{3r-3(s)}$, in a $Fe_{2.5}PO_4(OH)_{4.5}$ saturated solution (*Saturation Index* ($SI$) = 0). When assuming equilibrium for the $Fe_rPO_4(OH)_{3r-3(s)}$ phase in this system as well, the $LogIAP_{Fe_rPO_4(OH)_{3r-3}}$ equals the $LogK_{Fe_rPO_4(OH)_{3r-3}}$.

### 2.2. Batch experiments with natural groundwater

Aeration experiments with natural groundwater were done with groundwater collected from piezometers in an experimental field within the Hupsel brook catchment in the eastern part of the Netherlands (Van der Velde et al., 2010). The groundwater was sampled from two piezometers, gw3 and gw4, at a distance of 20 m from a drainage ditch (Van der Grift et al., 2014) during the summer of 2013. The filters of the piezometers were situated at one to three metres depth into the three metre thick sandy aquifer. The groundwater in this part of the experimental field is dominantly anoxic with Fe concentrations varying between 0.1 and 0.5 mmol $L^{-1}$, $PO_4$ concentrations between 6 and 50 μmol $L^{-1}$ and P/Fe ratios varying between 0.01 and 0.83 (Van der Grift et al., 2014). The collected water is representative for the anoxic groundwater seepage into surface water.

The groundwater was sampled with a peristaltic pump after first discarding at least three well volumes and no entrainment of bubbles was apparent in the tubes. The aqueous oxygen concentration, temperature and pH were measured on site. The anoxic water was directed into the bottom of 2 L glass bottles under continuous purging with $N_2$. Additionally, water samples for chemical analysis were also taken from the two piezometers. All samples were filtered through a 0.45 μm pore size cellulose nitrate filter. A sub-sample was collected in a polyethylene bottle and acidified to a pH of 1 using suprapur nitric acid (Inorganic Ventures). This sample was analysed for metals and total P by ICP-OES and Fe(II) using the ferrozine method (Viollier et al., 2000).

The anoxically sampled natural groundwater was transferred into the batch reactor by purging the bottle with $N_2$ while draining the water through a tube directly into the reactor purged with Ar. The oxidation experiment was initiated by changing the gas composition from Ar to a $CO_2$/pressurised air mixture. In contrast to the experiments with synthetic solution, the pH-stat device could not be used to derive Fe(II) oxidation rates due to the presence of dissolved carbonate in groundwater. The pH was not controlled by a pH stat device but the pH was constrained by the equilibrium between the $CO_2$ pressure and the inorganic carbon concentration. The required $CO_2$ content of the purging gas in order to maintain the in-situ pH was calculated with PHREEQC (Parkhurst and Appelo, 1999) from the measured pH and alkalinity. The pH of the solution was continuously monitored and did not change by more than 0.05 pH-values. Regularly, aliquots from the experimental solutions were taken and analysed as described in Section 2.1.1. Additional to the concentration measurements in the <0.45 μm filtrate, the 'truly' dissolved Fe(II), Fe(III) and $PO_4$ concentrations were measured after ultrafiltration of the <0.45 μm filtrates using membranes with nominal molecular weight cutoffs (MWCO) of 50 kDA (Amicon XM Polyacrylonitrile/PVC Copolymer membranes). For this, the <0.45 μm filtrates were immediately transferred into a 10 ml stirred ultrafiltration cell (Amicon 8010) and filtered with $N_2$ overpressure. It

should be noted that even a 50 kDa cutoff may not be sufficient to reliably isolate the truly dissolved fraction (50 kDa equals ≈50,000 atomic units, this are polymers with up to 500 $Fe(OH)_3$ units and a diameter up to a few nm). The obtained dissolved concentrations are still an upper estimate.

## 3. RESULTS

The results of the experiments with synthetic solutions are presented in the next sections for the experiments without $PO_4$, with an excess of P ($(P/Fe)_{ini} = 0.9$) and with an excess of Fe ($(P/Fe)_{ini} = 0.3$, 0.18 and 0.12), respectively. In each section first the reaction stoichiometry and, second, the reaction progress is presented. Examples of the reaction progress curves at a constant pH value of 6.1 and $O_2$ concentrations of 10.5 mg $L^{-1}$ are shown in Fig. 1 presenting the results from one experiment of a series of experiments with identical $(P/Fe)_{ini}$ ratios. Detailed results of all experiments are shown in the supplement (Figs. S2–S6) and summarised in Table 1. Finally, the results of the groundwater aeration experiments are presented.

### 3.1. Fe(II) oxidation experiments at $(P/Fe)_{ini} = 0$

#### 3.1.1. Reaction stoichiometry

The Fe(II) concentrations decreased over time after starting the aeration of the solution (Fig. 1) and this decrease was accompanied by the production of protons. The time evolution of the dissolved Fe(II) concentration at different pH values and $O_2$ concentrations are shown in Fig. S2, Row A. For the $PO_4$-free experiments, the $H^+/Fe^{2+}$ ratio equalled 1.90–1.94 and a good match was obtained between the progress of Fe(II) oxidation, calculated from the NaOH consumption, and discrete measurements of Fe(II) concentrations throughout these experiments (Table 1, Fig. S2, Row A). That is, the $H^+/Fe^{2+}$ ratio remained constant throughout the whole experiment. The experimentally derived $H^+/Fe^{2+}$ ratio closely matched the ideal stoichiometry of Fe(II) oxidation by oxygen in combination with Fe oxyhydroxide precipitation, i.e. 2 moles of protons were released per mole $Fe(OH)_3$ being formed.

#### 3.1.2. Reaction progress

The experiments without $PO_4$ had in common that the rates of Fe(II) oxidation were slow during the first tens of minutes and, subsequently, the rates went through a phase of acceleration. Afterwards, rates continuously slowed down upon consumption of reactants and finally approached completion after several hundreds of minutes (Figs. 1, S2, Row B). The target $O_2$ concentration was reached in less than ten minutes after the start of the experiment. During this period, an acceleration of the oxidation rate can be attributed to the build-up of the $O_2$ concentration. The increase of the reaction rate continued, however, up to several tens of minutes for the experiment at pH = 6.1 and $O_2$ = 10.5 mg $L^{-1}$ to over 100 min for exp. pH = 6.1, $O_2$ = 8.5 mg $L^{-1}$ and exp. pH = 6.4, $O_2$ = 3.6 mg $L^{-1}$. This extended period of acceleration could, therefore, not be attributed to the adjustment of $O_2$ concentrations in the reactor. The existence of distinct stages in the reaction progress is most apparent when using log-linear plots (Figs. 1, S2, Row C). After the initial stage, Fe(II) oxidation followed first-order kinetics which is reflected in a linear trend in the log-linear plots. The apparent rate constant was obtained from the slope of a linear regression line and varied between 0.0039 and 0.0053 $min^{-1}$ (Table 1, Fig. S2). The measured rate constants were a factor 1.3–1.6 higher than those derived from the rate law established by Stumm and Lee (1961).

### 3.2. Fe oxidation experiments at $(P/Fe)_{ini} = 0.9$

#### 3.2.1. Reaction stoichiometry

The $PO_4$ and Fe(II) concentrations decreased over time after starting the aeration of the solution. The Fe(II) consumption rate was, however, higher than the $PO_4$ consumption rate (Figs. 1, S3, Row A). When the Fe(II) oxidation approached completion, the $PO_4$ concentration remained around 60–80 μmol $L^{-1}$ irrespective of the oxygen concentration. The concomitant consumption of dissolved $PO_4$ and Fe(II) confirmed the formation of a Fe hydroxyphosphate precipitate during Fe(II) oxidation. It was possible to reproduce the time evolution of measured Fe(II) concentrations from the continuously recorded NaOH addition by optimising a constant molar $H^+/Fe^{2+}$ ratio for the P/Fe = 0.9 experiments (Figs. 1, S3, Row A). The molar $H^+/Fe^{2+}$ ratios were lower than for the $PO_4$-free experiments and equalled 1.33 and 1.27 for the three experiments at pH = 6.1 and pH = 6.4, respectively (Table 1, Fig. S3, Row A). In replicate experiments at pH = 6.1 and $O_2$ = 10.5 mg $L^{-1}$ identical $H^+/Fe^{2+}$ ratios were obtained. Also the molar $(P/Fe)_{ppt}$ ratio of the precipitates stayed relatively constant after the initial stage of the experiments. Deviation from this ratio during the initial stage of the experiment can be attributed to analytical inaccuracy as the decrease in Fe (II) and $PO_4$ concentrations was only around 10 μmol $L^{-1}$ or less. The $(P/Fe)_{ppt}$ ratios were, with values around 0.6, similar for all experiments at pH = 6.1 and slightly lower (0.56) for the experiment at pH = 6.4 (Table 1). A Fe hydroxyphosphate with a molar P/Fe ratio of 0.60 has the stoichiometry $Fe_{1.67}PO_4(OH)_{2.01}$ and one with a molar P/Fe ratio of 0.56 has the stoichiometry of $Fe_{1.79}PO_4(OH)_{2.37}$.

Model calculations give a molar $H^+/Fe^{2+}$ ratio of 1.31 during precipitation of a $Fe_{1.67}PO_4(OH)_{2.01}$ phase from an aerated solution with a $(P/Fe)_{ini}$ ratio of 0.9 and a pH = 6.1. This calculated ratio matches the experimentally observed ratio of 1.33 almost perfectly. A similar good match was obtained for the other experiment with a $(P/Fe)_{ini}$ ratio of 0.9 (Table 1). In addition, the time evolution of $PO_4$ concentrations, as calculated from the NaOH addition, the molar $H^+/Fe^{2+}$ ratio and the $(P/Fe)_{ppt}$ ratio were consistent with the $PO_4$ concentrations measurement on discrete samples, too. Hence, the alternative approaches for deriving the $(P/Fe)_{ppt}$ ratios yielded consistent results: at high $(P/Fe)_{ini}$ ratios the precipitating solid can be represented by an empirical stoichiometry of $Fe_{1.67}PO_4(OH)_{2.01}$ to $Fe_{1.79}PO_4(OH)_{2.37}$ and the stoichiometry did not seem to change throughout the reaction.

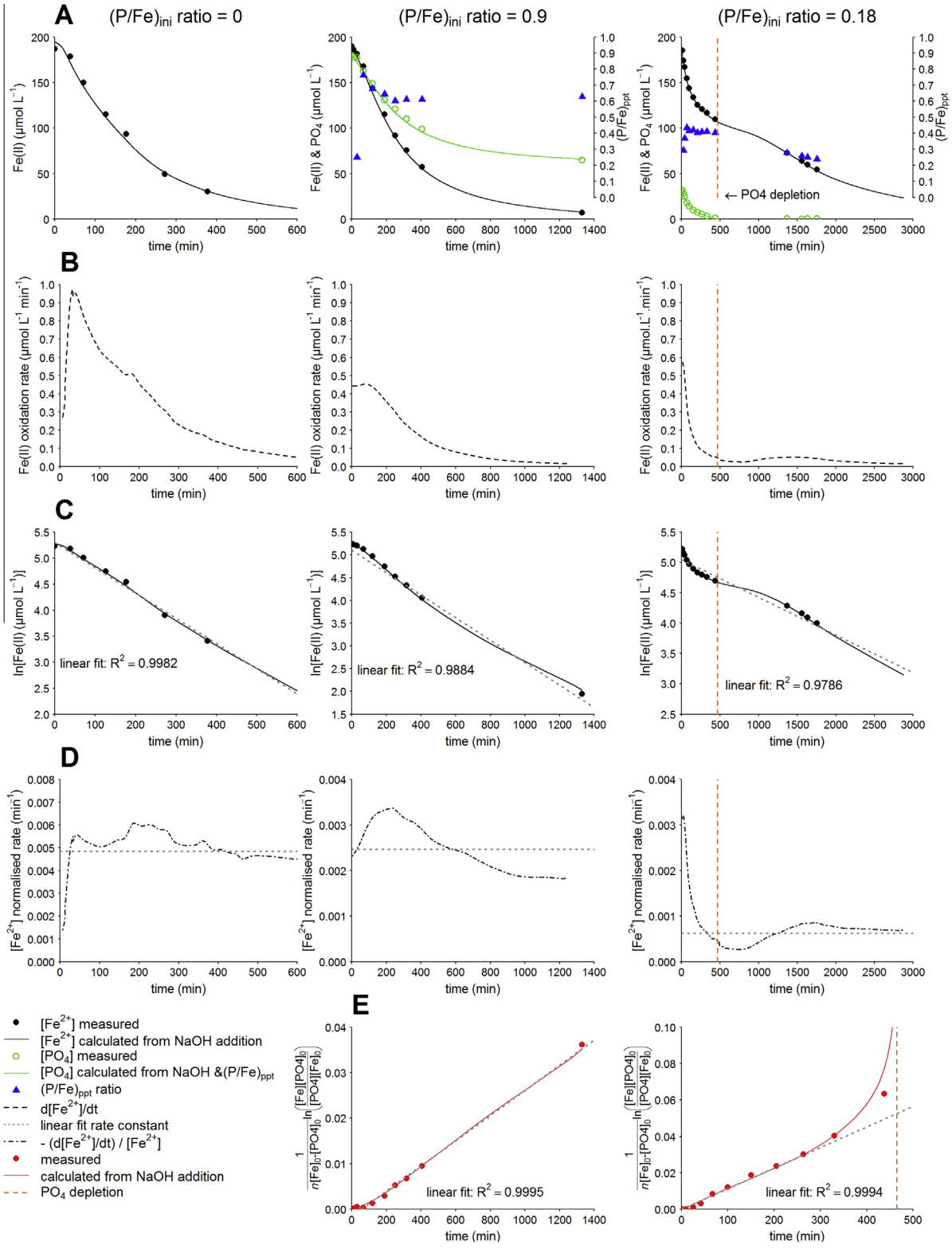


Fig. 1. Examples of the time evolution of Fe(II) oxidation during aeration experiments with $(P/Fe)_{ini}$ ratios of 0.9, 0.18 and 0 at pH = 6.1 and $O_2 = 10.5$ mg $L^{-1}$. Row A: Fe(II), PO4 concentration and $(P/Fe)_{ppt}$ ratio of precipitate. Row B: Fe(II) oxidation rate. Row C: semi logarithmic plot of the time evolution of Fe(II) concentration. Row D: Fe(II) normalised rates as a function of time. Row E: plot of the integrating the second-order rate law term versus time. For the experiment at $(P/Fe)_{ini} = 0.18$ only data before $PO_4$ depletion are plotted. Symbols are measurements on discrete samples. Solid lines are computed from the continuously monitored NaOH addition.

*3.2.2. Reaction progress*

Similar to the $PO_4$-free experiments, the course of the reaction can be divided into two stages with different Fe(II) oxidation kinetics. The existence of an initial reaction stage is most apparent when plotting the Fe(II) oxidation rate as function of time (Figs. 1, S3, Row B). During the initial reaction stage (to ≈200 min) the Fe(II) oxidation rate increased with time. This initial acceleration of the rates was also observed in the experiments in the absence of $PO_4$. However, the initial stage lasted longer in the presence of excess $PO_4$ compared with the $PO_4$-free experiments. During the second stage (after ≈200 min), the rate decreased with time.

The Fe(II) oxidation rates were lower in the $PO_4$ excess experiments compared with the $PO_4$-free experiments (Fig. 1, row B). For example, at a Fe(II) concentration of 100 μmol $L^{-1}$ in the experiment at pH = 6.1 and $O_2$ = 10.5 mg $L^{-1}$, the Fe(II) oxidation rate was 0.54 μmol $L^{-1}$ $min^{-1}$ in the absence of $PO_4$. In comparison, the rates were 0.32–0.34 μmol $L^{-1}$ $min^{-1}$ in the experiments with $(P/Fe)_{ini}$ ratios of 0.9 at the same Fe(II) and $O_2$ concentration. This trend also persisted at a lower $O_2$ concentration ($O_2$ = 3.6 mg $L^{-1}$): at the same Fe(II) concentration in the experiments at pH = 6.4, the rate was 0.57 μmol $L^{-1}$ $min^{-1}$ without $PO_4$ compared with 0.22 μmol $L^{-1}$ $min^{-1}$ in presence of $PO_4$.

In contrast to the $PO_4$-free experiments, the reaction did not follow pseudo-first-order kinetics after the initial acceleration phase when $PO_4$ was present. Although the decrease of $ln[Fe^{2+}]$ showed an almost linear trend with time after ≈200 min (Figs. 1, S3, Row C) the overall order of the reaction is not 1. The $[Fe^{2+}]$ normalised rates decreased after ≈200 min (Figs. 1, S3, Row D) but the deviation from first-order kinetics becomes apparent when plotting the logarithmised reaction rates (ln(v)) as a function of the logarithmised $Fe^{2+}$ concentrations ($ln[Fe^{2+}]$) (Fig. 2, top row). In the absence of $PO_4$, ln(v) decreased linearly with decreasing $ln[Fe^{2+}]$ with a slope of about 1. When $PO_4$ was present, the slope of the trend line was significantly steeper. That is, the apparent pseudo-first-order rate constant decreased after the initial stage (after ≈200 min) when $PO_4$ was present while it remains unchanged in the $PO_4$-free experiments. Hence, the results indicate that $PO_4$ concentrations influence Fe(II) oxidation rates in addition to temperature, $O_2$ concentration, Fe(II) concentration and pH.

### 3.3. Fe oxidation experiments with $(P/Fe)_{ini}$ = 0.3, 0.18 and 0.12

*3.3.1. Reaction stoichiometry*

The experiments with $(P/Fe)_{ini}$ ratios of 0.3, 0.18 and 0.12 have in common that $PO_4$ was virtually removed from solution before Fe(II) oxidation reached completion (Figs. 1, S4–S6, Row A). In contrast to the experiments

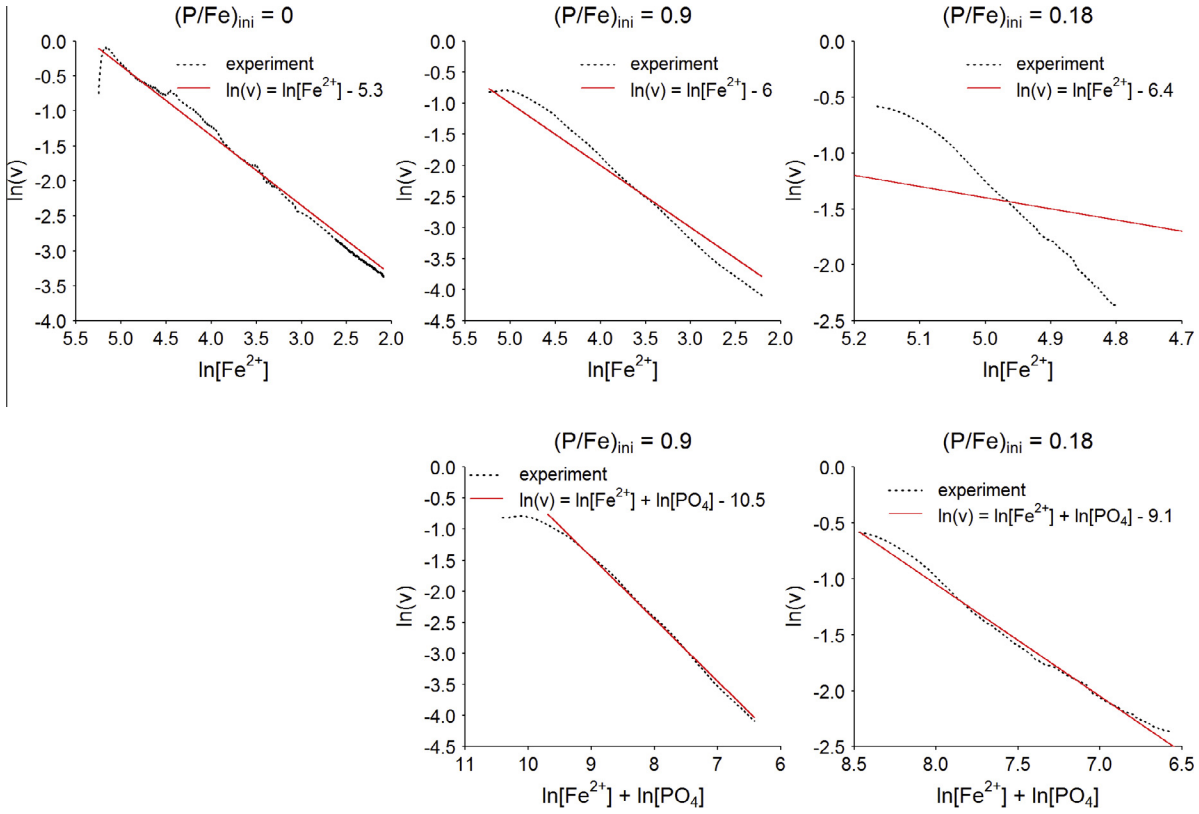


Fig. 2. Logarithmised Fe(II) oxidation rates of experiments with $(P/Fe)_{ini}$ ratio of 0, 0.9 and 0.18 at pH = 6.1 and $O_2$ = 10.5 mg $L^{-1}$ against the logarithmised Fe(II) concentrations (top row) and against the sum of the logarithmised Fe(II) and $PO_4$ concentrations (bottom row). Units in μmol $L^{-1}$. The red lines indicate a logarithmised Fe(II) oxidation rate with a slope of 1. (For interpretation of the references to colour in this figure legend, the reader is referred to the web version of this article.)

without $PO_4$ and higher $(P/Fe)_{ini}$ ratios, an initial stage with retarded Fe(II) oxidation was not noticeable. Nevertheless, the progress of Fe(II) oxidation exhibited two major stages: stage 1 where $PO_4$ is present in solution and the Fe(II) oxidation led to formation of Fe hydroxyphosphates and stage 2, after almost complete $PO_4$ removal from solution, when Fe(II) oxidation resulted in precipitation of Fe oxyhydroxide. The $(P/Fe)_{ppt}$ ratio of the Fe hydroxyphosphates that were formed during reaction stage 1, as calculated from the decrease in aqueous Fe(II) and $PO_4$ concentrations, varied only to a minor extent in the course of the reaction. When comparing experiments with different $(P/Fe)_{ini}$ ratios and pH, however, the $(P/Fe)_{ppt}$ ratios were not similar but varied between 0.38 and 0.48 (Table 1). A decrease of the $(P/Fe)_{ini}$ ratio from 0.3 to 0.12 resulted in a 0.06–0.09 lower $(P/Fe)_{ppt}$ ratio. In experiments conducted at pH 6.4, the $(P/Fe)_{ppt}$ ratios were similar (for $(P/Fe)_{ini} = 0.12$) or 0.04–0.05 units lower (for $(P/Fe)_{ini} = 0.18$ and 0.3) compared to experiments at pH 6.1. This resulted in $r$ values between 2.08 and 2.78 for the Fe hydroxyphosphate $Fe_rPO_4(OH)_{3r-3(s)}$.

The molar $H^+/Fe^{2+}$ ratio during reaction stage 1 varied between 1.42, for a precipitate with a $(P/Fe)_{ppt}$ ratio of 0.48, and 1.55 for a precipitate with a $(P/Fe)_{ppt}$ ratio of 0.41 (Table 1). The measured molar $H^+/Fe^{2+}$ ratios for the individual experiments agreed with the molar $H^+/Fe^{2+}$ ratios that were obtained from modelling the formation of Fe hydroxyphosphates with the experimentally derived $(P/Fe)_{ppt}$ ratio. The continuous Fe(II) curve, calculated with the $H^+/Fe^{2+}$ ratio from the recorded NaOH addition, traced the discretely measured Fe(II) concentrations during reaction stage 1. A similar good match was also found between the measured $PO_4$ concentrations and the $PO_4$ concentrations obtained from the recorded NaOH addition. This indicates that the $(P/Fe)_{ppt}$ ratio stayed practically constant in the various experiments as long as $PO_4$ was present in solution but varied between experiments with different initial conditions. After $PO_4$ was virtually depleted, the molar $H^+/Fe^{2+}$ ratios increased to values between 1.84 and 1.95 indicating that an Fe oxyhydroxide precipitated during the second stage of the reaction.

### 3.3.2. Reaction progress

Despite the absence of an initial reaction stage with retarded Fe(II) oxidation rates, the course of the reaction can be divided into different stages. During the first reaction stage with decreasing $PO_4$ concentrations, Fe(II) oxidation rates slowed down and exhibited a period of retardation when $PO_4$ was virtually depleted. After the Fe(II) oxidation rates had reached a minimum, they accelerated intermediately. Eventually, consumption of Fe(II) caused a decrease of the reaction rate during the experimental trajectory after $PO_4$ depletion (Fig. 3). Depending on the $(P/Fe)_{ini}$ ratio, a minimum in the reaction rate was reached within ≈45 to ≈460 min after the moment of $PO_4$ depletion (Fig. 3, Table 1). The time interval between $PO_4$ depletion and the minimum in Fe(II) oxidation rate was longest for the experiment with the $(P/Fe)_{ini}$ ratio of 0.3 and shortest for the experiment with the $(P/Fe)_{ini}$ ratio of 0.12. The intermittent increase in reaction rate was most pronounced for the experiment with $(P/Fe)_{ini} = 0.12$ and pH = 6.4 (from 0.11 to 0.32 μmol $L^{-1}$ $min^{-1}$) and smallest for the experiments with $(P/Fe)_{ini} = 0.3$ and pH = 6.1 (from 0.018 to 0.030 μmol $L^{-1}$ $min^{-1}$). At equal $(P/Fe)_{ini}$ ratios, the increase was larger for the experiments at pH values of 6.4 than at pH values of 6.1.

The shift in Fe(II) oxidation kinetics during the reaction is distinct and visible when plotting the time evolution of the rates on log-linear scale (Figs. 1, S4–S6. Row C). During the presence of aqueous $PO_4$, the $[Fe^{2+}]$ normalised rates decreased up to an order of magnitude (Figs. 1, S4–S6. Row D). When plotting the ln(v) as a function of the $ln[Fe^{2+}]$ the slope of the trend line was much steeper than 1 (Fig. 2, top row). This indicates that the reaction kinetics

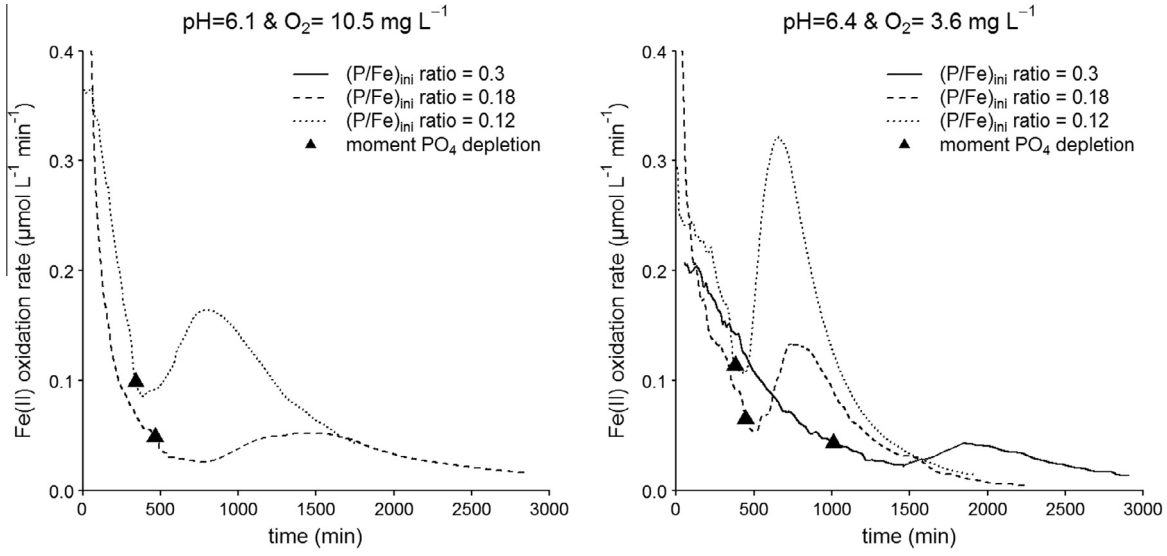


Fig. 3. Fe(II) oxidation rate during aeration experiments with initial aqueous P/Fe ratios of 0.3, 0.18 and 0.12. The P/Fe 0.12 experiment started with higher initial Fe(II) concentrations than the P/Fe 0.3 and 0.18 experiments.

are not pseudo-first-order but the decrease of $PO_4$ affected the Fe(II) oxidation rate as well.

After $PO_4$ depletion and acceleration of Fe(II) oxidation rate, $[Fe^{2+}]$ normalised rates stayed virtually constant. Hence, after $PO_4$ depletion, Fe(II) oxidation followed first-order kinetics. The related first-order rate constant ranged from 0.0007 to 0.0023 $min^{-1}$ for the reaction stage after $PO_4$ depletion (Table 1). These values are lower than the first-order rate constants obtained from $PO_4$-free experiments (0.0049–0.0053 $min^{-1}$) and also lower than the rate constant derived from Stumm and Lee (1961) at the same pH and $O_2$ conditions (0.0030–0.0040 $min^{-1}$).

### 3.4. Groundwater aeration experiments

The aqueous composition of groundwater sampled from the Hupsel field can be characterised as anoxic fresh water with near-neutral pH (Table S1). Iron concentrations ranged from 175 to 188 μmol $L^{-1}$ and $PO_4$ concentrations ranged from 5.8 to 11.3 μmol $L^{-1}$, leading to aqueous P/Fe ratios from 0.037 to 0.073. These P/Fe ratios were in the lower range of the previously observed P/Fe ratios in the groundwater (van der Grift et al., 2014). The DOC concentrations varied between 35 and 41.2 mg $L^{-1}$. In order to increase the $(P/Fe)_{ini}$ ratio, two experiments were spiked with 20 μmol $L^{-1}$ $KH_2PO_4$ before the start of aeration (Table 2).

Aeration of the anoxic groundwater caused a decrease in Fe(II) concentrations, usually to values below 5 μmol $L^{-1}$ over the duration of the experiments (Fig. 4). In the experiments gw3.2 and gw4.2, initial Fe(III) concentrations were 15 and 24 μmol $L^{-1}$, respectively, indicating that some Fe (II) oxidation had occurred before the start of the experiment. Phosphate concentrations before spiking were 2 and 3 μmol $L^{-1}$ lower than the concentrations measured in the field samples, implying that some $PO_4$ immobilisation had occurred as well.

During the first hours of the aeration experiment, $PO_4$ concentrations decreased until they stabilised around values of 4–5 μmol $L^{-1}$ for experiment gw3.1 and gw4.1 and of 20–22 μmol $L^{-1}$ for experiment gw3.2 and gw4.2. This fast decrease in the beginning of the experiment was comparable with the decrease as observed in the experiments with synthetic solutions. A remarkable difference was, however, that in the experiments with the synthetic solution virtually all aqueous $PO_4$ was removed from solutions while in the groundwater aeration experiments $PO_4$ remained in solution although $PO_4$ was not in excess. After about 24 h reaction time, the $PO_4$ concentrations stabilised at a level that was higher for the $PO_4$-spiked experiment compared with that for the unspiked experiments. Another difference to the experiments with synthetic solutions was that Fe(III) was also detected in solution. Dissolved Fe(III) concentration reached levels of 40–55, 80, 70–75 and 90 μmol $L^{-1}$ for experiment gw3.1, gw4.1, gw3.2 and gw4.2, respectively. It is most likely that this Fe(III) is not truly dissolved but that stable $PO_4$-rich Fe(III) colloids were formed which were able to pass through the 0.45 μm filter membranes.

The 'dissolved' (<0.45 μm) Fe(III) and $PO_4$ concentrations were stable for up to 44 days with Fe(III) concentrations between 79 and 94 μmol $L^{-1}$ and $PO_4$ concentrations of 3.6–4.1 μmol $L^{-1}$ for the non-amended experiments and 21 μmol $L^{-1}$ for the two spiked experiments (Table 2). Between 62% and 85% of the initially dissolved $PO_4$ ended in the <0.45 μm fraction. This fraction accounted for between 37% and 55% of total Fe (Fig. 4).

The chemical compositions of the colloidal and particulate phase differed from each other. The P/Fe ratio of the <0.45 μm fraction was higher than that of the particulate fraction that had not passed the 0.45 μm filters. After all Fe(II) had been oxidised, the $(P/Fe)_{ppt}$ ratio of the particulate fraction was lower than the $(P/Fe)_{ini}$ ratio while the $(P/Fe)_{ppt}$ ratio of the <0.45 μm fraction was higher than the $(P/Fe)_{ini}$ ratio (Table 2).

For experiment gw4.2, the 'truly' dissolved Fe(II), Fe (III) and $PO_4$ concentrations were measured additionally after ultrafiltration with 50 kDa membranes. The 'truly' dissolved (<50 kDa) Fe(II) and colloidal (<0.45 μm, >50 kDa) Fe(III) concentrations during the experiment were similar to the total dissolved Fe(II) and Fe(III) concentrations, respectively. This implies that Fe in the colloidal fraction dominated the total dissolved concentrations at the end of the experiments (Fig. 4D).

During the first 5 h of experiment gw4.2, less than 30% of the initial Fe(II) was transformed into colloidal Fe(III). This transformation was accompanied by an almost complete transition of 'truly' dissolved $PO_4$ into colloidal $PO_4$ (Fig. 4D). Quantitative fixation of $PO_4$ in colloidal form coupled to partial oxidation of the initially present Fe(II) resulted in high $(P/Fe)_{colloid}$ ratios during this period. The $(P/Fe)_{colloid}$ ratio was about 0.45 after 5 h, which is comparable with the $(P/Fe)_{ppt}$ ratios of precipitates formed in the synthetic water experiments with excess of Fe(II). During the first 5 h of this experiment, the colour intensity of the filter residues on the 50 kDa filters increased while the appearance of the residue on the 0.45 μm filters did not change over this period (Fig. S7). This is another indication for the predominant formation of colloids during this experimental period. The partitioning of $PO_4$ between particulate (>0.45 μm), colloidal and truly dissolved fractions did not show significant shifts between 5 h and 48 h reaction time. A small increase in the particulate $PO_4$ fraction together with a decrease in the colloidal $PO_4$ fraction was observed after 48 h. The colloidal Fe(III) concentration continued to increase after near-depletion of truly dissolved $PO_4$ up to 24 h and was stable afterwards up to the end of the experiment. After complete Fe(II) oxidation, about 85% of the initial aqueous $PO_4$ ended in the colloidal fraction and this resulted in a colloidal phase with a (P/Fe) ratio almost twice the $(P/Fe)_{ini}$ ratio.

## 4. DISCUSSION

### 4.1. P/Fe ratios of the Fe hydroxyphosphate precipitate

The first objective of our study was to determine the $(P/Fe)_{ppt}$ ratios in Fe hydroxyphosphates that form during Fe(II) oxidation in synthetic $PO_4$ containing solutions as a function of pH, the aqueous $(P/Fe)_{ini}$ ratio and the reaction progress. The pH and the $(P/Fe)_{ini}$ ratio in solution

Table 2
Overview of groundwater aeration experiments.

| Sample | $PO_4$ spiked | pH exp. | $Fe^{2+}$ initial | $PO_4$ initial | $(P/Fe)_{ini}$ | $Fe^{3+}$ diss. initial | $Fe^{3+}$ diss. final | $PO_4$ diss. final | First-order rate constant | (P/Fe) ratio colloidal fraction | (P/Fe) ratio particulate fraction |
|---|---|---|---|---|---|---|---|---|---|---|---|
| | μmol $L^{-1}$ | | μmol $L^{-1}$ | μmol $L^{-1}$ | | μmol $L^{-1}$ | μmol $L^{-1}$ | μmol $L^{-1}$ | $min^{-1}$ | | |
| gw3.1 | – | 6.1 | 169 | 5.7 | 0.033 | 9 | 84 (at 888 h.) | 3.6 | 0.0018 | 0.085 | 0.017 |
| gw4.1 | – | 5.9 | 185 | 7.0 | 0.038 | 2 | 79 (at 1056 h.) | 4.1 | 0.0012 | 0.057 | 0.029 |
| gw3.2 | 20 | 6.1 | 161 | 31 | 0.19 | 15 | 93 (at 576 h.) | 21 | 0.0021 | 0.28 | 0.11 |
| gw4.2 | 20 | 6.0 | 158 | 25 | 0.16 | 24 | 94 (at 146 h.) | 21 | 0.0019 | 0.24 | 0.03 |

influence the $(P/Fe)_{ppt}$ ratios of the precipitates forming from homogeneous solution: with decreasing $(P/Fe)_{ini}$ ratios and increasing pH, $(P/Fe)_{ppt}$ ratios decrease. Interestingly, measured $H^+/Fe^{2+}$ ratios and $(P/Fe)_{ppt}$ ratios did not change detectably throughout the experiments although the P/Fe ratios of the solutions changed due to either superproportional removal of $PO_4$ in the $(P/Fe)_{ini} = 0.3$, 0.18 and 0.12 experiments or superproportional removal of Fe(II) in the $(P/Fe)_{ini} = 0.9$ experiments. Hence, the chemical composition of the Fe hydroxyphosphate seems to be determined during the initial stage of Fe(II) oxidation, which may be considered as the nucleation stage of the precipitate formation sequence. This suggests that the initially formed precipitates function as a template for Fe hydroxyphosphates precipitating at the particle surfaces as a consequence of surface catalytic Fe(II) oxidation. A small but detectable decrease in $(P/Fe)_{ppt}$ ratios with decreasing $(P/Fe)_{ini}$ ratios has been observed in precipitates formed in excess of Pleading to exclusive formation of Fe(III)-phosphate (Voegelin et al., 2013; Senn et al., 2015; Châtellier et al., 2013). Voegelin et al. (2013) performed a time-resolved aeration experiment with a synthetic solution with a $(P/Fe)_{ini}$ ratio of 0.29. In their experiments, the $(P/Fe)_{ppt}$ ratio of the formed precipitate decreased from ≈0.6 to ≈0.52 during Fe(II) oxidation in presence of $PO_4$. This ratio is higher than obtained in our experiments at a $(P/Fe)_{ini}$ ratio of 0.3 (0.48 and 0.44 at pH values of 6.1 and 6.4, respectively), and we observed no decline of the $(P/Fe)_{ppt}$ ratios to such an extent and no detectable change in the $H^+/Fe^{2+}$ ratio during the experiment. However, the $(P/Fe)_{ppt}$ values we obtain from the loss of dissolved Fe (II) and $PO_4$ are reflecting the average composition of the precipitates. Formation of precipitates with lower $(P/Fe)_{ppt}$ ratios, when approaching $PO_4$ depletion in solution, might not lead to a significant shift in the average $(P/Fe)_{ppt}$ values when the difference in $(P/Fe)_{ppt}$ ratio is small and the relative contribution to the total amount of precipitate is small. Furthermore, in our experiments the pH was kept constant over time by 0.01 M NaOH titration. Although rapid stirring was used to minimize local pH maxima, it cannot be excluded that locally elevated pH may favour Fe(III) hydrolysis over $PO_4$ complexation and may lead to lower $(P/Fe)_{ppt}$ ratios than observed in experiments performed in pH-buffered solutions. In contrast to our experiments, the pH was not maintained constant in the experiments by Voegelin et al. (2013). Hence, the shift in $(P/Fe)_{ppt}$ ratios during their experiments could also be attributed to the drifting pH value.

Recent studies show that electrolyte cations like $Na^+$ and $Ca^{2+}$ can enter amorphous Fe hydroxyphosphates and, therefore, affect the OH/Fe ratio of the precipitate (Châtellier et al., 2013; Senn et al., 2015). Châtellier et al. (2013) reported a $(Na/Fe)_{ppt}$ ratio up to ≈0.2 at pH 6.0. In our experiments, we used $K^+$ as background electrolyte and $NH_4^+$ is added with the Fe(II) stock solution. Like $Na^+$ these cations may enter the precipitate and affect P/Fe and OH/Fe ratios. Based on charge balance, uptake of $Na^+$ in a precipitate with a $(Na/Fe)_{ppt}$ ratio of 0.2 increases the molar $H^+/Fe^{2+}$ ratio with 0.2. Our PHREEQC calculated molar $H^+/Fe^{2+}$ ratios do not differ to such an extent from

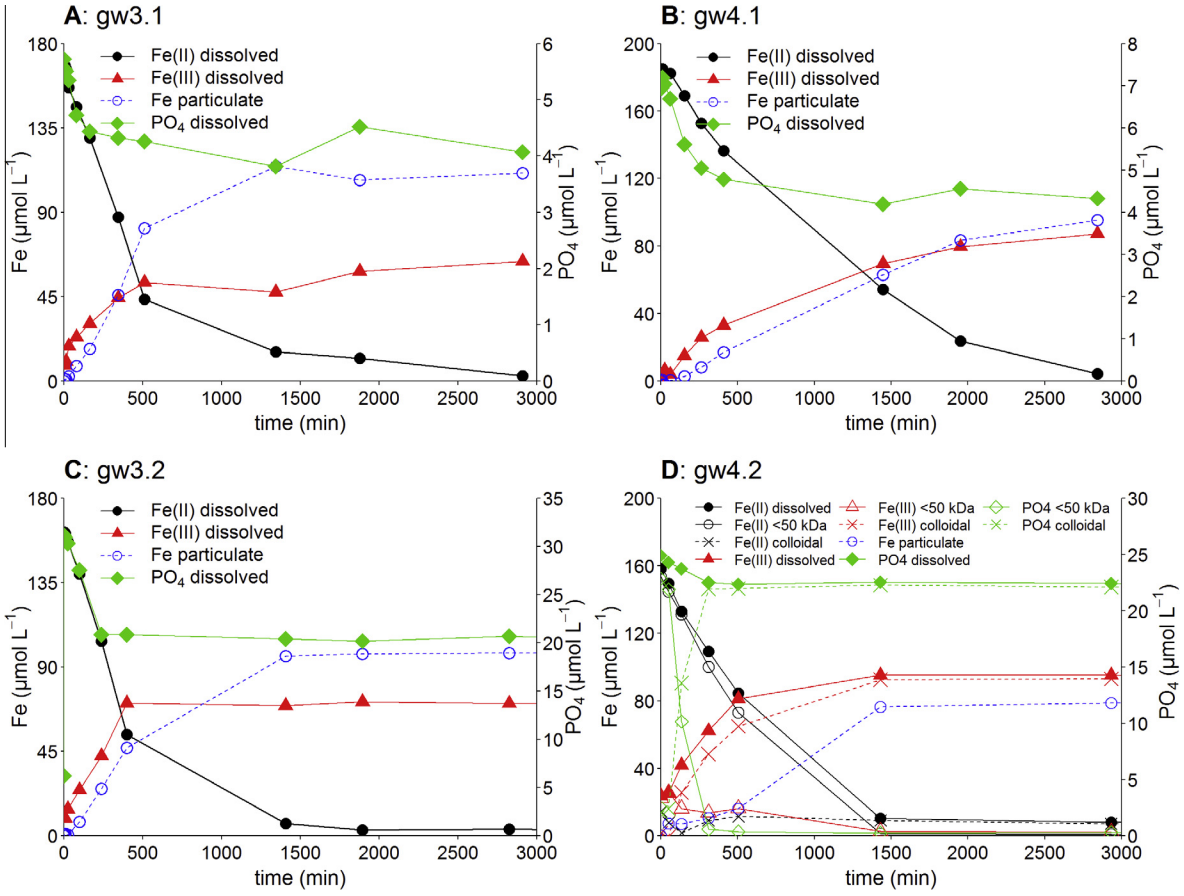


Fig. 4. Measured Fe(II), Fe(III) and $PO_4$ concentrations (<0.45 µm) and calculated particulate Fe concentrations during groundwater aeration experiments (A) gw3.1, (B) gw4.1, (C) gw3.2 and (D) gw4.2. Plot (D) gives also the measured truly dissolved concentrations (<50 kDA) and calculated colloidal concentrations (<0.45 µm and >50 kDA).

the measured molar $H^+/Fe^{2+}$ ratio (Table 1). This indicates that incorporation of other cations into the Fe hydroxyphosphates is of minor relevance in our experiments. The experiments of Châtellier et al. (2013) were conducted at much higher initial $Fe^{2+}$ concentrations than our experiments (5 mmol $L^{-1}$ compared to ≈0.2 mmol $L^{-1}$) as well as higher background electrolyte concentration (133 mmol $L^{-1}$ NaCl compared to 4.8 mmol $L^{-1}$ KCl). In particular the higher background electrolyte concentration might be the reason why incorporation of other cations is observed in the experiments by Châtellier et al. (2013).

Our experimental results with $(P/Fe)_{ini}$ ratios of 0.9 are in line with earlier work that concluded that $PO_4$ uptake per oxidised Fe is limited to a solid P/Fe ratio of ≈0.5–0.6 (Tessenow, 1974; Gunnars et al., 2002; Roberts et al., 2004; Voegelin et al., 2010). Voegelin et al. (2013) reported an increase of the $(P/Fe)_{ppt}$ ratio from 0.56 to 0.72 upon increase of the $(P/Fe)_{ini}$ ratio from 0.55 to 1.91 and concluded that increasing $(P/Fe)_{ini}$ ratios above 0.55 affects $(P/Fe)_{ppt}$ ratio only to a minor extent. A similar result was reported by Châtellier et al. (2013). Although many arrangements of Fe octahedrons and $PO_4$ tetrahedrons in primary building blocks may yield to formation of Fe hydroxyphosphates with a maximal $(P/Fe)_{ppt}$ of ≈0.5, the appearance of this maximum $(P/Fe)_{ppt}$ ratio is supported by the nucleation and growth mechanism of Fe oxyhydroxides in presence of $PO_4$ as postulated by Rose et al. (1996) based on EXAFS analyses. Rose et al. (1996) concluded that presence of chloride and $PO_4$ as ligands in Fe(III) dimers inhibits the linkage of other Fe(III) octahedra through double corner sharing. These complexes, consisting of two Fe octahedrons and one $PO_4$ tetrahedron, form then the building blocks in the continuation of polymerisation. Dependent on the $(P/Fe)_{ini}$ ratio, further growth occurs through association of such small units through $PO_4$ bridges, which results in a precipitate with a solid P/Fe ratio of ≈0.5 or by bridging the basic units through Fe single-corner sharing, which generates lower $(P/Fe)_{ppt}$ ratios (Rose et al., 1996).

Other studies provide indications that the stoichiometry of the building blocks might be different when amorphous Fe(III) phosphates are synthesized at elevated $(P/Fe)_{ini}$ and high total P and Fe concentrations (Voegelin et al., 2010) or at low pH (Mikutta et al., 2014). In precipitates with P/Fe ratios close to 1.0, double-corner sharing Fe (III) dimers are absent in the structure. This suggests that

monomeric Fe(III) complexes serve as building blocks for the formation of Fe(III) phosphates under the corresponding conditions. Hence, the model proposed by Rose et al. (1996) might provide an explanation for the formation of precipitates with $(P/Fe)_{ppt}$ values roughly around 0.5 for a relatively wide range of $(P/Fe)_{ini}$ values in our experiments. However, the model is not of general validity and does not imply the formation of a distinct stoichiometric phase.

### 4.2. Kinetics of Fe(II) oxidation

The second objective of our study was to establish the kinetics of Fe(II) oxidation upon aeration of synthetic solutions with varying $(P/Fe)_{ini}$ ratios. Our experiments show that presence of dissolved $PO_4$ exerts influence on the rates of Fe(II) oxidation. In general, Fe(II) oxidation proceeds slower in the presence of dissolved $PO_4$ but decrease of the $PO_4$ concentration during Fe(II) oxidation due to the formation of Fe hydroxyphosphates causes additional deceleration.

#### *4.2.1. Kinetics of Fe(II) oxidation in phosphate free experiments*

The pseudo-first-order Fe(II) oxidation rate constants in our experiments are a factor 1.3–1.6 higher than those derived for the rate law established by Stumm and Lee (1961). This may be the result of the lower initial Fe(II) concentration that were used in the experiments of Stumm and Lee (1961) (50 μmol $L^{-1}$) which likely results in lower surface catalysis, or by the higher ionic strength in their experiments due to the use of the bicarbonate buffer to control the pH which reduces the Fe(II) oxidation rate (Sung and Morgan, 1980). In the absence of $PO_4$, Fe(II) oxidation rates increase during the initial stage for the experiments. Occurrence of an initial stage with retarded Fe(II) oxidation rates has been reported by Vollrath et al. (2012) and the increase in rates after the initial state has been attributed to surface catalysis by the accumulation of Fe oxyhydroxides. Vollrath et al. (2012) argued that surface catalysis might also affected the Fe(II) oxidation rates measured by Stumm and Lee (1961) and that their rate law might not represent exclusively homogeneous Fe(II) oxidation. In this case, the initial stage reflects the period of Fe oxyhydroxide nucleation until surface catalysis of Fe(II) oxidation coupled to particle growth becomes the dominant pathway. Surface catalysis is well documented for Fe(II) oxidation. Sung and Morgan (1980) concluded that surface catalytic Fe(II) oxidation is only observed in experiments with a pH of 7 and higher. However, Pedersen et al. (2005) showed that Fe(II) can interact with Fe oxyhydroxides surfaces and surface-bound Fe(II) can be oxidised at pH 6.5. When surface catalysis is affecting Fe(II) oxidation rates the structure and properties of the precipitate are expected to exert influence on the rates among other factors. The background electrolyte composition and concentration may influence the precipitate properties. Differences in pH control (pH-stat in our experiments versus bicarbonate buffer used by Stumm and Lee, 1961) may lead to different precipitates and, therefore, to differences in Fe(II) oxidation rates.

#### *4.2.2. Dependency of Fe(II) oxidation kinetics on phosphate*

The overall dependency of Fe(II) oxidation rates on $PO_4$ concentrations demonstrate the ambivalent effect of $PO_4$ on Fe(II) oxidation kinetics. This effect is observed when comparing the time required to oxidise 75% of the initially added Fe(II) ($t_{3/4}$). The shortest $t_{3/4}$ values are obtained for experiments with $PO_4$-free solutions. In experiments with $(P/Fe)_{ini}$ values between 0.12 and 0.3, the $t_{3/4}$ values increase with increasing $PO_4$ concentration but with $(P/Fe)_{ini} = 0.9$, the $t_{3/4}$ is shorter than in the experiments with lower $(P/Fe)_{ini}$ values (Table 1). In earlier work on Fe(II) oxidation in presence of $PO_4$ it was reported that dissolved $PO_4$ accelerates the oxidation of aqueous Fe(II) in homogenous systems (Tamura et al., 1976; Mitra and Matthews, 1985; Mao et al., 2011) but slows down oxidation of adsorbed Fe(II) in heterogeneous systems (Wolthoorn et al., 2004). The acceleration of homogenous Fe(II) oxidation in the presence of $PO_4$ may be an explanation for the less pronounced or not noticeable initial stage with retarded Fe(II) oxidation rates during our experiments with $(P/Fe)_{ini}$ ratios greater than zero. The general trend in our experiments is, however, that Fe(II) oxidation rates are lower in the presence of $PO_4$ than in $PO_4$-free solutions. Based on the consideration that heterogeneous oxidation is the dominant pathway for Fe(II) oxidation after the initial phase, our observations agree with those of Wolthoorn et al. (2004). That is, $PO_4$ reduces the rate of surface catalysed Fe(II) oxidation which is the dominant mechanism for Fe(II) oxidation after the initial stage of experiments in the presence as well as in the absence of $PO_4$. Hence, the general trend that addition of $PO_4$ slows down Fe(II) oxidation rates could be ascribed to a weaker catalytic effect of Fe hydroxyphosphates compared to Fe oxyhydroxides.

This mechanism alone, however, cannot account for the shorter $t_{3/4}$ at $(P/Fe)_{ini} = 0.9$ compared with $t_{3/4}$ values of experiments with $(P/Fe)_{ini} = 0.12$, 0.18 and 0.3. In the experiments with $(P/Fe)_{ini} = 0.3$ and lower, $PO_4$ becomes depleted before 75% of the added Fe(II) is oxidised. Phosphate depletion is followed by a period of delayed Fe(II) oxidation rates and the length of the timeframe between the moment of $PO_4$ depletion and minimum in Fe(II) oxidation rate increases with increasing $(P/Fe)_{ini}$ ratios (Table 1). This phenomenon additionally controls the $t_{3/4}$. When $(P/Fe)_{ini} = 0.9$, $PO_4$ is in excess and an intermediate period of delayed Fe(II) oxidation is absent. As a consequence, $t_{3/4}$ is shorter at $(P/Fe)_{ini} = 0.9$. Relating Fe(II) oxidation rates and $PO_4$ concentration is further complicated by the observation that, against the general trend of delaying Fe(II) oxidation upon $PO_4$ addition, removal of $PO_4$ upon progressing reaction decelerates the reaction within one experiment. This phenomenon is addressed in more detail below.

Dissolved $PO_4$ might affect Fe(II) oxidation by multiple mechanisms: changing the speciation of dissolved Fe(II), influencing the nucleation of iron precipitates, and interfering with surface catalysis by changing the surface speciation of the Fe hydroxyphosphates. Consequently, the dependency of the rates on $PO_4$ concentration might vary in the different stages of the reaction. The complexity of the dependency on $PO_4$ concentration becomes obvious when

plotting ln(v) as a function of ($\ln[Fe^{2+}] + \ln[PO_4]$) (Fig. 2, bottom row). At the beginning of the reaction, the curves do not follow a linear trend, but in a later phase a linear function with a slope of 1 resembles the experimentally derived results well. Hence, a pseudo-second-order rate law provides a good description of the progress of Fe(II) oxidation in the presence of $PO_4$ when surface catalysis is the dominant pathway:

$$\frac{d[Fe^{2+}]}{dt} = -k_2[Fe^{2+}][PO_4] \quad (5)$$

where [i] refers to the concentration of species i, $k$ denotes the reaction rate constant. We may reformulate Eq. (5) in terms of reacted Fe(II) at time $t$, with a standard reaction progress parameter $\xi$. Then $[Fe^{2+}] = [Fe^{2+}]_0 - \xi$ and $[PO_4] = [PO_4]_0 - n\xi$, where $n$ is the stoichiometric $(P/Fe)_{ppt}$ ratio of the Fe hydroxyphosphate. Then, the expression of the rate law becomes:

$$-\frac{d\xi}{dt} = -k_2([Fe^{2+}]_0 - \xi)([PO_4]_0 - n\xi) \quad (6)$$

In Eq. (6) we assume that the reaction rate is first-order with respect to the total $PO_4$ concentration. Integration between $t = 0$ (when $\xi = 0$) and $t$, the time of interest, yields:

$$\int_0^{\xi} \frac{d\xi}{([Fe^{2+}]_0 - \xi)([PO_4]_0 - n\xi)} = k_2 \int_0^{t} dt \quad (7)$$

The integrated rate equation is:

$$\frac{\ln(\xi - [Fe^{2+}]_0) - \ln([PO_4]_0 - n\xi) - \ln(-[Fe^{2+}]_0) + \ln([PO_4]_0)}{n[Fe^{2+}]_0 - [PO_4]_0} = k_2 t \quad (8)$$

Upon rearrangement of the integrated rate equation, this becomes:

$$\ln\left(\frac{[Fe^{2+}][PO_4]_0}{[PO_4][Fe^{2+}]_0}\right) = k_2(n[Fe^{2+}]_0 - [PO_4]_0)t \quad (9)$$

For all four experiments with an $(P/Fe)_{ini}$ ratio of 0.9 the plot of $\frac{1}{n[Fe^{2+}]_0 - [PO_4]_0} \ln\left(\frac{[Fe^{2+}][PO_4]_0}{[PO_4][Fe^{2+}]_0}\right)$ versus time yields a straight line after the initial stage (Figs. 1, S3, Row E). Hence, progress of the reaction can be described using a pseudo-second-order rate law with first-order dependencies on $PO_4$ and Fe(II). The pseudo-second-order rate constant for the experiments with a $(P/Fe)_{ini}$ ratio of 0.9 can be obtained from the slope of a linear regression line and varies between $1.53 \times 10^{-5}$ and $2.78 \times 10^{-5}$ μmol$^{-1}$ L min$^{-1}$ (Table 1). Pseudo-second-order kinetics can also describe the progress of Fe(II) oxidation in the experiments with lower $(P/Fe)_{ini}$ ratios during the first reaction stage wherein $PO_4$ is present. Application of Eq. (9) gives a satisfactorily description of the reaction until the $PO_4$ concentrations fall to a level that ranges from 7% to 18% of the initial $PO_4$ concentration (2.1 and 9.5 μmol L$^{-1}$) (Figs. 1, S4–S6, row E). Pseudo-second-order rate constants vary between $5.72 \times 10^{-5}$ and $1.13 \times 10^{-4}$ μmol$^{-1}$ L min$^{-1}$ (Table 1). The pseudo-second-order rate constants, obtained from the integrated rate law, match the $y$-intercept from the linear trend line in the ln(v) versus ($\ln[Fe^{2+}] + \ln[PO_4]$) plots (Fig. 2).

Tamura et al. (1976) and Mao et al. (2011) studied Fe(II) oxidation in the presence of excess $PO_4$ and concluded that the kinetics are first order with respect to dissolved $PO_4$ concentration. Tamura et al. (1976) proposed following rate law:

$$\frac{d[Fe]}{dt} = -k[OH^-][O_2][Fe][H_2PO_4^-]^n \quad (10)$$

with $k = 5.02 \times 10^9$ M$^{-3}$ s$^{-1}$, $n = 1$ for $H_2PO_4^- < 0.1$ mol L$^{-1}$ and $k = 5.02 \times 10^{10}$ M$^{-4}$ s$^{-1}$, $n = 1$ for $H_2PO_4^- >$ 0.1 M.

For the experimental conditions pH = 6.1, $O_2$ = 10.5 mg L$^{-1}$ and $[PO_4]_{ini} = 0.0002$ mol L$^{-1}$ the rate law of Tamura et al. (1976) gives pseudo-second-order rate constants of $1.24 \times 10^{-6}$ μmol$^{-1}$ L min$^{-1}$ and for the experimental condition pH = 6.4, $O_2 = 3.6$ mg L$^{-1}$ and $[PO_4]_{ini} = 0.0002$ mol L$^{-1}$, a value of $0.85 \times 10^{-6}$ μmol$^{-1}$ L min$^{-1}$ is obtained. These values are lower compared with our experimentally derived second-order rate constants. Mao et al. (2011) reported even lower reaction rates but they investigated systems with nanomolar Fe concentrations in which surface catalysis is less important and homogeneous oxidation dominates. They concluded that the aqueous $FePO_4^-$ complex is the most reactive phosphate complex and due to its higher abundance than the aqueous $Fe(OH)_2$ complex the $FePO_4^-$ complex is the most important Fe(II) species contributing to the overall rate of Fe (II) oxygenation at circumneutral pH. Although Fe(II) oxidation is most likely predominantly heterogeneous in our experiments and $(P/Fe)_{in}$ ratios are much lower, the effect of phosphate on Fe(II) speciation and formation of reactive Fe(II)-phosphate complexes in solution or at the solid surface may also provide an explanation for the observed first-order dependency of Fe(II) oxidation rate on $PO_4$ concentration.

#### 4.2.3. Kinetics of Fe(II) oxidation after phosphate depletion

The Fe(II) oxidation rates increase after $PO_4$ depletion and the Fe(II) oxidation kinetics become first-order with respect to the Fe(II) concentration at fixed pH and oxygen conditions (Table 1, Figs. S4–S6, Row C). Voegelin et al. (2013) reported an increase of Fe(II) oxidation rates after $PO_4$ depletion as well. Based on data published by Wolthoorn et al. (2004), Voegelin et al. (2013) suggested that this can be ascribed to stronger catalytic properties of Fe oxyhydroxide surfaces compared with the surfaces of Fe hydroxyphosphates. Our results support this interpretation which can also explain the differences in Fe(II) oxidation rates in experiments with $(P/Fe)_{ini}$ ratios of 0.12, 0.18 and 0.3 after $PO_4$ depletion. Even when $PO_4$ is consumed, Fe(II) oxidation rates in experiments with $PO_4$ are lower than those in $PO_4$-free experiments and, hence, depend on the history of the system. When comparing the time between the moments of $PO_4$ depletion and minimal Fe(II) oxidation rate or when comparing the extent of intermittent increase in reaction rate after $PO_4$ depletion, it turns out that the Fe(II) oxidation rate accelerates faster

in experiments with lower $(P/Fe)_{ini}$ ratios (Table 1). Additionally, the first-order rate constants after $PO_4$ depletion are generally lower than those obtained from $PO_4$-free experiments and decrease with increasing $(P/Fe)_{ini}$ (Table 1). Hence, the amount of the initially formed Fe hydroxyphosphate or its $(P/Fe)_{ppt}$ ratio affects the kinetics of continuing Fe(II) oxidation after $PO_4$ depletion. In other words, the phases formed before and after $PO_4$ depletion are not completely independent from each other. Voegelin et al. (2013) found that about half of newly formed Fe(III) after $PO_4$ depletion contributes to the polymerisation of initially precipitated Fe hydroxyphosphate into $PO_4$-rich Fe oxyhydroxides with a maximum P/Fe ratio of 0.25. The other half of the formed Fe(III) precipitates as poorly-crystalline lepidocrocite. That is, the initially formed Fe hydroxyphosphate acts as a sink for Fe(III) which is formed after $PO_4$ depletion. In this case, the amount of Fe hydroxyphosphate determines how much of newly formed Fe(III) becomes available for the formation of lepidocrocite. This mechanism may explain the dependency of Fe(II) oxidation rates after $PO_4$ depletion on $(P/Fe)_{ini}$: at low $(P/Fe)_{ini}$ only small amounts of Fe hydroxyphosphate are formed and more Fe(III) can be channelled towards lepidocrocite. At high $(P/Fe)_{ini}$ less Fe(III) is available for the precipitation as lepidocrocite. Based on observations by Wolthoorn et al. (2004) we assume that lepidocrocite is a more potent surface catalyst than Fe hydroxyphosphates. The dependency of the pseudo-first-order rate constant after $PO_4$ depletion on $(P/Fe)_{ini}$ and the extent of Fe(II) oxidation rates after $PO_4$ consumption can then be attributed to the different extent of lepidocrocite formed per oxidised Fe (II) after $PO_4$ depletion.

#### *4.2.4. Dependency of Fe(II) oxidation kinetics on oxygen concentration and pH*

The rate law for Fe(II) oxidation, as established by Stumm and Lee (1961), is second-order with respect to $[OH^-]$ while the rate law by Tamura et al. (1976) is first-order with respect to the $[OH^-]$ when phosphate is present. According to both rate laws, the reaction is first-order with respect to oxygen concentration. First-order dependency on oxygen concentration is supported by our experimental results. Increasing the oxygen concentration by a factor of 0.7 leads to an increase in the pseudo-second-order rate constant by a factor of about 0.6 (experiment at $pH = 6.1$, $O_2 = 8.5$ mg $L^{-1}$; $k = 1.53 \times 10^{-5}$ μmol$^{-1}$ L min$^{-1}$, experiments at $pH = 6.1$, $O_2 = 10.5$ mg $L^{-1}$; $k = 2.48 \times 10^{-5} - 2.78 \times 10^{-5}$ μmol$^{-1}$ L min$^{-1}$).

We have not systematically explored the dependency of the reaction kinetics on pH, but comparing reaction rates obtained at pH 6.1 and pH 6.4 does shed some light on the pH dependency of Fe(II) oxidation in the presence of $PO_4$ in our experiments. Experiments at pH 6.1 and pH 6.4 were not performed at the same oxygen concentration, and therefore, the dependency of the rates on oxygen concentration has to be taking into consideration. In the experiments at $pH = 6.4$ and $O_2 = 3.6$ mg $L^{-1}$, the $[OH^-]$ is twice as high but the $O_2$ concentration is almost three times lower compared to the experiments at $pH = 6.1$ and $O_2 = 10.5$ mg $L^{-1}$. Second-order dependency on $[OH^-]$ would lead to 33% larger rates at $pH = 6.4$ and $O_2 = 3.6$ mg $L^{-1}$ compared with rates at $pH = 6.1$ and $O_2 = 10.5$ mg $L^{-1}$. If the kinetic reaction is first-order with respect to $[OH^-]$, 32% lower rates would be expected. For experiments with $(P/Fe)_{ini}$ ratios of 0.9, 0.3, 0.18 and 0.12, the pseudo-second-order rate constants obtained at $pH = 6.4$ and $O_2 = 3.6$ mg $L^{-1}$ are between 33% and 27% lower than rate constants at $pH = 6.1$ and $O_2 = 10.5$ mg $L^{-1}$. The increase in rates upon increasing the pH from 6.1 to 6.4 is lower than expected from the oxidation kinetics in the absence of $PO_4$. The change in rates is proportional to the increase in $[OH^-]$ and this supports the findings of Tamura et al. (1976) that Fe(II) oxidation kinetics in presence of $PO_4$ are first-order with respect to $[OH^-]$.

### 4.3. Phosphate immobilisation upon aeration of natural groundwater

The third objective of our study was to assess the effectiveness of the formation of Fe-$PO_4$ phases to immobilise $PO_4$ when natural Fe(II) and $PO_4$-containing groundwater is exposed to atmospheric oxygen. Our study shows that experiments with synthetic solutions are suitable to predict Fe(II) oxidation rates and $PO_4$ immobilisation dynamics upon aeration of natural groundwater: Fe(II) oxidation initially results in the formation of a Fe hydroxyphosphate phase until $PO_4$ is virtually depleted and afterwards Fe(II) oxidation leads to precipitation of a Fe oxyhydroxide phase.

Due to the presence of dissolved carbonate, the pH-stat device could not be used to continuously derive Fe(II) oxidation rates during the aeration experiments with natural groundwater. However, the measured decrease of logarithmised Fe(II) concentration during the groundwater aeration experiments (Fig. 5) is well predicted by using the rate laws parameterised with results from experiments with synthetic solutions. For this, the decrease of the Fe(II) concentration with time was calculated by using a combination of the second-order-rate law (before $PO_4$ depletion) and first-order rate law (after $PO_4$ depletion) with rate constants taken from experiments with synthetic solutions under conditions that most closely match those of the groundwater experiments ($(P/Fe)_{ini}$ ratio = 0.12, $pH = 6.1$ and $O_2 = 10.5$ mg $L^{-1}$). In contrast, Fe(II) oxidation rates are overestimated when using the first-order rate law with a rate constant from $PO_4$-free synthetic solution experiments. Hence, the effects of $PO_4$ on Fe(II) oxidation kinetics in natural groundwater experiments are comparable to those of experiments in synthetic solutions. Based on interpolation of the concentration measurements, values for $t_{3/4}$ fall into the range of 600–1500 min which is somewhat lower than the synthetic water experiments at $(P/Fe)_{ini} = 0.12$ and 0.18 (900–1800 min). It is known that the presence of other constituents such as carbonate, silicic acid, DOC and alkaline earth metals may also influence the Fe(II) oxidation rate (e.g. Pullin and Cabaniss, 2003; Wolthoorn et al., 2004). As shown by Wolthoorn et al. (2004), surface catalysed oxidation of Fe(II) proceeds slower in presence of silica than in its absence, but rates are still a factor 2 higher than in a $PO_4$-containing solution. The presence of silicate

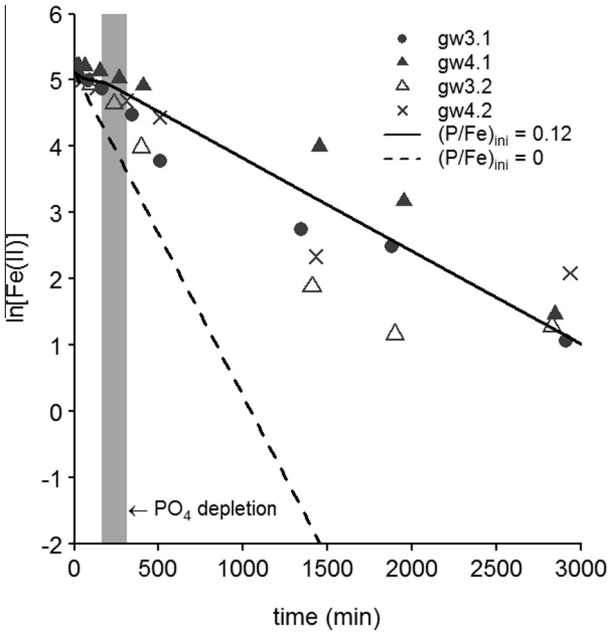


Fig. 5. Measured logarithmised Fe(II) concentrations (μmol $L^{-1}$) as a function of time during groundwater aeration experiments. The lines represents the predicted time evolution of logarithmised Fe(II) concentrations (μmol $L^{-1}$) based on (1) a combination of the 2nd rate law constant before $PO_4$ depletion and 1st order rate law constant after $PO_4$ depletion obtained from the synthetic solution experiment with a $(P/Fe)_{ini}$ ratio = 0.12 and pH = 6.1 and (2) the parameterised 1st order rate law obtained from the synthetic solution experiment in the absence of $PO_4$ ($(P/Fe)_{ini}$ ratio = 0).

in groundwater may explain the slightly lower $t_{3/4}$ values in experiments with natural groundwater compared with synthetic solutions. At longer times (>2500 s), the observed Fe (II) concentrations seem to approach a steady state level which is higher than the detection limit (data not shown). Pullin and Cabaniss (2003) observed a similar feature of inhibited Fe(II) oxidation in the presence of fulvic acid after longer reaction times. They explained this feature by the formation of stable Fe(II) organic complexes and chemical reduction of Fe(III) by DOM.

A remarkable difference between experiments with natural groundwater and synthetic solutions is that Fe(II) oxidation results in the formation of stable $PO_4$-rich colloids while in the experiments with synthetic solutions the precipitates agglomerate and flocculate. The formation of stable $PO_4$-rich iron colloids can be attributed to the chemical composition of the groundwater (Table S1), that has relatively high DOC concentrations (30–40 mg $L^{-1}$ expressed as NPOC) and low salinity (chloride concentrations from 18 to 33 mg $L^{-1}$). Colloidal Fe(III) particles can be stabilised against aggregation in the presence of DOC (Pizarro et al., 1995; Pullin and Cabaniss, 2003; Gaffney et al., 2008; Neal et al., 2008). Low ionic strength favours the stability of colloidal suspensions as electrostatic repulsion between equally charged colloidal particles can be attenuated at high ionic strength (Gunnars et al., 2002; Mosley et al., 2003). Furthermore, $PO_4$ itself has a positive effect on the colloidal stability (He et al., 1996) but presence of $PO_4$ alone, as shown by the low Fe(III) concentration of the filtrates of the experiments with synthetic solutions, appears not to be sufficient to suppress coagulation (Fig. S1).

### 4.4. Predictive modelling of $PO_4$ immobilisation during groundwater seepage

The applicability of our experimental results for predicting $PO_4$ immobilisation during groundwater seepage was further evaluated by modelling the experimentally derived data of $PO_4$ immobilisation of groundwater aeration experiments from the study of Griffioen (2006). The residual $PO_4$ concentrations after aeration were modelled based on solubility calculations with Eq. (4). The experimentally observed critical $(P/Fe)_{ini}$ value at which $PO_4$ remains dissolved after complete Fe(II) oxidation is well reproduced when assuming that a homogeneous Fe hydroxyphosphate phase is formed with a molar ratio of ≈0.6 ($Fe_{1.67}PO_4(OH)_{2.01}$) (Fig. 6). Below that ratio, $PO_4$ concentrations in 0.45 μm filtered solutions are within a range of 1.5–10.5 μmol $L^{-1}$ at the end of the aeration experiments. In these solutions, total-Fe concentrations are detected within a range of 2.5–35 μmol $L^{-1}$ after 1 day of aeration. This indicates that, similar to our groundwater experiments, these measured Fe and $PO_4$ concentrations can be ascribed to the presence of colloidal particles. For the groundwater samples with $(P/Fe)_{ini}$ values from ≈0.6 to 1.5, a good resemblance is obtained between the experimental $PO_4$ concentration after aeration and the modelled $PO_4$ concentration after precipitation of $Fe_{1.67}PO_4(OH)_{2.01}$.

For the majority of groundwater samples with $(P/Fe)_{ini} > 1.5$, more $PO_4$ immobilisation occurred than could be explained by precipitation of Fe hydroxyphosphates. The experiments with $(P/Fe)_{ini} > 1.5$ and little $PO_4$ immobilisation also show small decrease of Ca concentrations. This indicates that formation of Ca phosphates, Ca carbonates and/or Ca–Fe–phosphates, which is induced by degassing of the groundwater, contributes to the removal of dissolved $PO_4$ in experiments with substantial $PO_4$ immobilisation and $(P/Fe)_{ini} > 1.5$. The role of $PO_4$ co-precipitation with Ca precipitates in $PO_4$ immobilisation has been demonstrated by Griffioen (2006) and Senn et al. (2015).

Up to initial aqueous P/Fe ratios of 1.5, precipitation of a Fe hydroxyphosphate phase with P/Fe ratio of 0.6 can be used for predictive modelling of fast (<1 day) $PO_4$ immobilisation upon aeration of anoxic natural groundwater. The groundwater samples from the experiments of Griffioen (2006) with $(P/Fe)_{ini}$ ratios >1.5 can all be considered as nutrient-rich ($PO_4 > 50$ μmol $L^{-1}$). The occurrence of nutrient-rich groundwater in the Netherlands is limited to the Holocene coastal lowland areas (Griffioen et al., 2013) and nutrient-rich groundwater is usually not found in Pleistocene areas. As an illustration, 79% of the groundwater samples from the Dutch National Groundwater Quality Monitoring Network (Van Duijvenbooden et al., 1985) taken between 2000 and 2009 have P/Fe ratios <1.5. Hence, a model based on the precipitation of an Fe hydroxyphosphate with a $(P/Fe)_{ppt}$ of ≈0.6 seems suitable to estimate

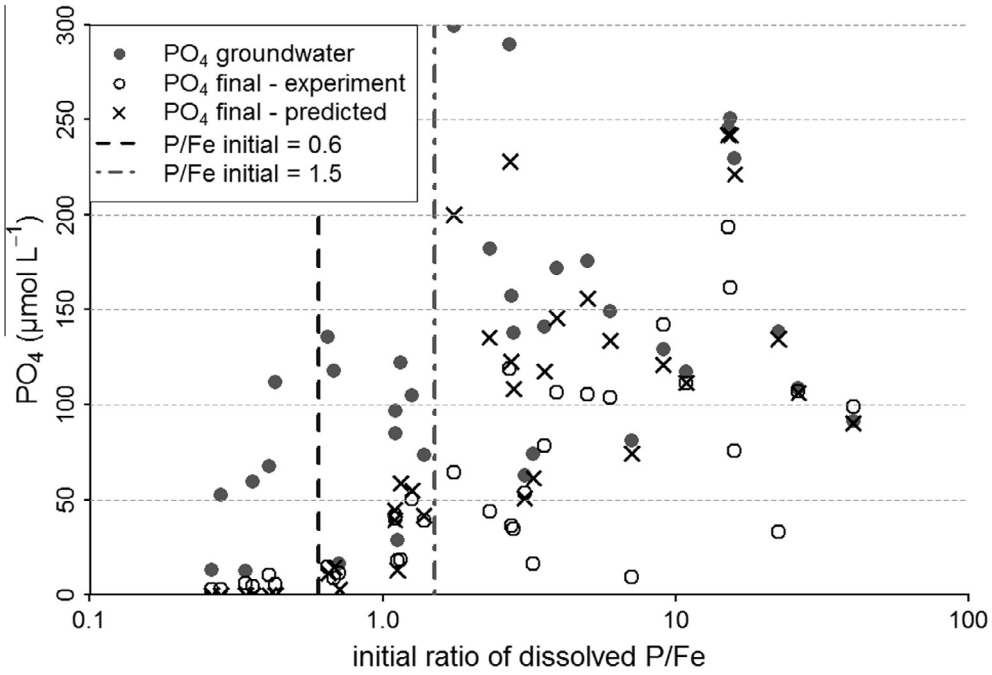


Fig. 6. Measured and predicted $PO_4$ concentrations against the $(P/Fe)_{ini}$ ratio from groundwater aeration experiments; experimental results as published by Griffioen (2006) and model results for precipitation of a Fe hydroxyphosphate with a solid molar P/Fe ratio of 0.6.

$PO_4$ removal during Fe(II) oxygenation in a wide range of streams, ditches and channels that receive anoxic Fe-rich groundwater. These findings provide a solid basis for further studies on transport and bioavailability of $PO_4$ in surface water systems.

## 5. CONCLUSIONS

Aeration experiments with Fe(II) containing solutions demonstrate that dissolved $PO_4$ can be effectively immobilised in the form of an homogeneous Fe hydroxyphosphate. In the presence of dissolved $PO_4$, oxidation of Fe(II) leads to the formation of Fe hydroxyphosphates whose $(P/Fe)_{ppt}$ ratios remain virtually constant throughout the reaction despite the change in P/Fe ratio in the solution. However, the $(P/Fe)_{ppt}$ ratio varies depending on the $(P/Fe)_{ini}$ ratio and the pH value. Initial aqueous P/Fe ratios ranging from 0.12 to 0.9 result in $(P/Fe)_{ppt}$ ratios from 0.38 to 0.61. Experiments conducted at pH 6.4 form precipitates with P/Fe ratios that are slightly lower than those forming at pH 6.1.

Presence of dissolved $PO_4$ exerts influence on the rates of Fe(II) oxidation. In general, Fe(II) oxidation proceeds slower in the presence of dissolved $PO_4$ but, conversely, the decrease of the $PO_4$ concentration during Fe(II) oxidation due to the formation of Fe hydroxyphosphates causes additional deceleration of the reaction rate. Although the dependency of the reaction rates on $PO_4$ concentration might be complicated, the progress of the reaction in our experiments can be described using a pseudo-second-order rate law with first-order dependencies on both $PO_4$ and Fe(II) concentrations. The observed effect of pH on Fe(II) oxidation kinetics in in presence of $PO_4$ is smaller than in the absence of $PO_4$: the reaction appears to be first-order with respect to $[OH^-]$ in the presence of $PO_4$ while it is second-order in absence of $PO_4$. After $PO_4$ depletion, the Fe(II) oxidation rate increases again and the kinetics shift to a first-order process with respect to the Fe(II) concentration at constant pH and oxygen concentration. The first-order rate constants after $PO_4$ depletion are lower compared to those in $PO_4$-free solutions. This implies that the initially formed Fe hydroxyphosphate affects the kinetics of continuing Fe(II) oxidation after $PO_4$ depletion which is likely a result of transformation of the initially formed Fe hydroxyphosphate into other Fe phases during continuing Fe(II) oxidation.

Aeration experiments with natural groundwater show formation of Fe hydroxyphosphates during Fe(II) oxidation in presence of $PO_4$ and the progress of Fe(II) oxidation can be described with rate-laws obtained from experiments with synthetic solutions. However, the presence of DOC in the groundwater results in the formation of stable Fe hydroxyphosphate colloids that remain in suspension for longer periods. The formation of a Fe hydroxyphosphate phase with a molar P/Fe ratio of 0.6 can be used for predictive modelling of $PO_4$ immobilisation upon aeration of pH-neutral natural groundwater with an initial P/Fe ratio up to 1.5.

## ACKNOWLEDGEMENTS

Deirdre Clark is gratefully acknowledged for her contribution to the experimental work and field-work. Ype van der Velde is thanked for his mathematical assistance. We thank Andreas Voegelin for the helpful discussions and his suggestions for improvement of the manuscript. The useful comments of three anonymous reviewers are greatly appreciated. Funding of the project was provided by Deltares (project SO2015: From catchment to coast).

## APPENDIX A. SUPPLEMENTARY DATA

Supplementary data associated with this article can be found, in the online version, at http://dx.doi.org/10.1016/j.gca.2016.04.035.

## REFERENCES


Baken S., Sjöstedt C., Gustafsson J. P., Seuntjens P., Desmet N., De Schutter J. and Smolders E. (2013) Characterisation of hydrous ferric oxides derived from iron-rich groundwaters and their contribution to the suspended sediment of streams. *Appl. Geochem.* **39**, 59–68.

Baken S., Salaets P., Desmet N., Seuntjens P., Vanlierde E. and Smolders E. (2015a) Oxidation of iron causes removal of phosphorus and arsenic from streamwater in groundwater-fed lowland catchments. *Environ. Sci. Technol.* **49**, 2886–2894.

Baken S., Verbeeck M., Verheyen D., Diels J. and Smolders E. (2015b) Phosphorus losses from agricultural land to natural waters are reduced by immobilization in iron-rich sediments of drainage ditches. *Water Res.* **71**, 160–170.

Ball J. W. and Nordstrom D. K. (1991) *User's manual for wateq4f, with revised thermodynamic data base and text cases for calculating speciation of major, trace, and redox elements in natural waters, USGS Open-File Report: 91–183*. U.S Geological Survey Menlo Park, California, United States.

Bonneville S., Van Cappellen P. and Behrends T. (2004) Microbial reduction of iron(III) oxyhydroxides: effects of mineral solubility and availability. *Chem. Geol.* **212**, 255–268.

Buffle J., De Vitre R. R., Perret D. and Leppard G. G. (1989) Physico-chemical characteristics of a colloidal iron phosphate species formed at the oxic-anoxic interface of a eutrophic lake. *Geochim. Cosmochim. Acta* **53**, 399–408.

Châtellier X., Grybos M., Abdelmoula M., Kemner K. M., Leppard G. G., Mustin C., West M. M. and Paktunc D. (2013) Immobilization of P by oxidation of Fe(II) ions leading to nanoparticle formation and aggregation. *Appl. Geochem.* **35**, 325–339.

Cumplido J., Barron V. and Torrent J. (2000) Effect of phosphate on the formation of nanophase lepidocrocite from Fe(II) sulfate. *Clays Clay Miner.* **48**, 503–510.

Davison W. and Seed G. (1983) The kinetics of the oxidation of ferrous iron in synthetic and natural waters. *Geochim. Cosmochim. Acta* **47**, 67–79.

Deng Y. (1997) Formation of iron(III) hydroxides from homogeneous solutions. *Water Res.* **31**, 1347–1354.

Dzombak D. A. and Morel F. M. (1990) *Surface complexation modeling: hydrous ferric oxide*. Wiley, New York.

Einsele W. (1934) Über chemische und kolloidchemische Vorgänge in Eisen-Phosphat-Systemen unter limnochemischen und limnogeologischen Gesichtspunkten. *Arch. Hydrobiol.* **33**, 361–387.

Filippelli G. M. (2008) The global phosphorus cycle: past, present, and future. *Elements* **4**, 89–95.

Fox L. E. (1988) The solubility of colloidal ferric hydroxide and its relevance to iron concentrations in river water. *Geochim. Cosmochim. Acta* **52**, 771–777.

Fox L. E. (1989) A model for inorganic control of phosphate concentrations in river waters. *Geochim. Cosmochim. Acta* **53**, 417–428.

Frapporti G., Vriend S. P. and van Gaans P. F. M. (1993) Hydrogeochemistry of the shallow dutch groundwater: interpretation of the National Groundwater Quality Monitoring Network. *Water Resour. Res.* **29**, 2993–3004.

Fytianos K., Voudrias E. and Raikos N. (1998) Modelling of phosphorus removal from aqueous and wastewater samples using ferric iron. *Environ. Pollut.* **101**, 123–130.

Gaffney J. W., White K. N. and Boult S. (2008) Oxidation state and size of Fe controlled by organic matter in natural waters. *Environ. Sci. Technol.* **42**, 3575–3581.

Griffioen J., Vermooten S. and Janssen G. (2013) Geochemical and palaeohydrological controls on the composition of shallow groundwater in the Netherlands. *Appl. Geochem.* **39**, 129–149.

Griffioen J. (1994) Uptake of phosphate by iron hydroxides during seepage in relation to development of groundwater. *Environ. Sci. Technol.* **28**, 675.

Griffioen J. (2006) Extent of immobilisation of phosphate during aeration of nutrient-rich, anoxic groundwater. *J. Hydrol.* **320**, 359–369.

Gunnars A., Blomqvist S., Johansson P. and Andersson C. (2002) Formation of Fe(III) oxyhydroxide colloids in freshwater and brackish seawater, with incorporation of phosphate and calcium. *Geochim. Cosmochim. Acta* **66**, 745–758.

He Q. H., Leppard G. G., Paige C. R. and Snodgrass W. J. (1996) Transmission electron microscopy of a phosphate effect on the colloid structure of iron hydroxide. *Water Res.* **30**, 1345–1352.

Heiberg L., Koch C. B., Kjaergaard C., Jensen H. S. and Hansen H. C. B. (2012) Vivianite precipitation and phosphate sorption following iron reduction in anoxic soils. *J. Environ. Qual.* **41**, 938–949.

Hug S. J., Leupin O. X. and Berg M. (2008) Bangladesh and Vietnam: different groundwater compositions require different approaches to arsenic mitigation. *Environ. Sci. Technol.* **42**, 6318–6323.

Hyacinthe C. and Van Cappellen P. (2004) An authigenic iron phosphate phase in estuarine sediments: composition, formation and chemical reactivity. *Mar. Chem.* **91**, 227–251.

Iuliano M., Ciavatta L. and De Tommaso G. (2007) On the solubility constant of strengite. *Soil Sci. Soc. Am. J.* **71**, 1137–1140.

Kaegi R., Voegelin A., Folini D. and Hug S. J. (2010) Effect of phosphate, silicate, and Ca on the morphology, structure and elemental composition of Fe(III)-precipitates formed in aerated Fe(II) and As(III) containing water. *Geochim. Cosmochim. Acta* **74**, 5798–5816.

Koroleff E. (1983) Determination of phosphorus. In *Methods of Seawater Analysis* (eds. K. Grasshoff, M. Ehrhardt and K. Kremling). Verlag Chemie, Weinheim, pp. 117–122.

Ler A. and Stanforth R. (2003) Evidence for surface precipitation of phosphate on goethite. *Environ. Sci. Technol.* **37**, 2694–2700.

Lienemann C. P., Monnerat M., Janusz D. and Perret D. (1999) Identification of stoichiometric iron-phosphorus colloids produced in a eutrophic lake. *Aquat. Sci. Res. Across Bound.* **61**, 133–149.

Luedecke C., Hermanowicz S. W. and Jenkins D. (1989) Precipitation of ferric phosphate in activated sludge: a chemical model and its verification. *Water Sci. Technol.* **21**, 325–337.

Mao Y., Pham A. N., Rose A. L. and Waite T. D. (2011) Influence of phosphate on the oxidation kinetics of nanomolar Fe(II) in aqueous solution at circumneutral pH. *Geochim. Cosmochim. Acta* **75**, 4601–4610.

Matthiesen H., Leipe T. and Laima M. (2001) A new experimental setup for studying the formation of phosphate binding iron oxides in marine sediments. Preliminary results. *Biogeochemistry* **52**, 79–92.

Mayer T. D. and Jarrell W. M. (2000) Phosphorus sorption during iron(II) oxidation in the presence of dissolved silica. *Water Res.* **34**, 3949–3956.

Mikutta C., Schröder C. and Marc Michel F. (2014) Total X-ray scattering, EXAFS, and Mössbauer spectroscopy analyses of

amorphous ferric arsenate and amorphous ferric phosphate. *Geochim. Cosmochim. Acta* **140**, 708–719.
Millero F. J. (1985) The effect of ionic interactions on the oxidation of metals in natural waters. *Geochim. Cosmochim. Acta* **49**, 547–553.
Mitra A. K. and Matthews M. L. (1985) Effects of pH and phosphate on the oxidation of iron in aqueous solution. *Int. J. Pharm.* **23**, 185–193.
Mosley L. M., Hunter K. A. and Ducker W. A. (2003) Forces between colloid particles in natural waters. *Environ. Sci. Technol.* **37**, 3303–3308.
Navrotsky A., Mazeina L. and Majzlan J. (2008) Size-driven structural and thermodynamic complexity in iron oxides. *Science* **319**, 1635–1638.
Neal C., Lofts S., Evans C. D., Reynolds B., Tipping E. and Neal M. (2008) Increasing iron concentrations in UK Upland Waters. *Aquat. Geochem.* **14**, 263–288.
Nriagu J. O. and Dell C. I. (1974) Diagenetic formation of iron phosphates in recent lake sediments. *Am. Mineral.* **59**, 934–946.
Nriagu J. O. (1972) Solubility equilibrium constant of strengite. *Am. J. Sci.* **272**, 476–484.
Parkhurst D. L. and Appelo C. (1999) *User's guide to phreeqc (Version 2): a computer program for speciation, batch-reaction, one-dimensional transport, and inverse geochemical calculations.* .
Pedersen H. D., Postma D., Jakobsen R. and Larsen O. (2005) Fast transformation of iron oxyhydroxides by the catalytic action of aqueous Fe(II). *Geochim. Cosmochim. Acta* **69**, 3967–3977.
Perret D., Gaillard J. F., Dominik J. and Atteia O. (2000) The diversity of natural hydrous iron oxides. *Environ. Sci. Technol.* **34**, 3540–3546.
Pizarro J., Belzile N., Filella M., Leppard G. G., Negre J.-C., Perret D. and Buffle J. (1995) Coagulation/sedimentation of submicron iron particles in a eutrophic lake. *Water Res.* **29**, 617–632.
Pratesi G., Cipriani C., Giuli G. and Birch W. D. (2003) Santabarbaraite: a new amorphous phosphate mineral. *Eur. J. Mineral.* **15**, 185–192.
Pullin M. J. and Cabaniss S. E. (2003) The effects of pH, ionic strength, and iron–fulvic acid interactions on the kinetics of non-photochemical iron transformations. I. Iron(II) oxidation and iron(III) colloid formation. *Geochim. Cosmochim. Acta* **67**, 4067–4077.
Roberts L. C., Hug S. J., Ruettimann T., Billah M., Khan A. W. and Rahman M. T. (2004) Arsenic removal with iron(II) and iron(III) in waters with high silicate and phosphate concentrations. *Environ. Sci. Technol.* **38**, 307–315.
Roden E. E. and Edmonds J. W. (1997) Phosphate mobilization in iron-rich anaerobic sediments: microbial Fe(III) oxide reduction versus iron-sulfide formation. *Arch. Hydrobiol.* **139**, 347–378.
Rose J., Manceau A., Bottero J. Y., Masion A. and Garcia F. (1996) Nucleation and growth mechanisms of Fe oxyhydroxide in the presence of $PO_4$ ions. 1. Fe K-edge EXAFS study. *Langmuir* **12**, 6701–6707.
Schoumans O. F. and Chardon W. J. (2014) Phosphate saturation degree and accumulation of phosphate in various soil types in The Netherlands. *Geoderma* **237**, 325–335.
Senn A. C., Kaegi R., Hug S. J., Hering J. G., Mangold S. and Voegelin A. (2015) Composition and structure of Fe(III)-precipitates formed by Fe(II) oxidation in water at near-neutral pH: interdependent effects of phosphate, silicate and Ca. *Geochim. Cosmochim. Acta* **162**, 220–246.
Stumm W. and Lee G. F. (1961) Oxygenation of ferrous iron. *Ind. Eng. Chem.* **53**, 143–146.
Stumm W. and Morgan J. J. (1970) *Aquatic Chemistry: An Introduction Emphasizing Chemical Equilibria in Natural Waters*, New York.
Stumm W. and Sigg L. (1979) Kolloidchemische grundlagen der phosphor-elimination in fallung, flockung und filtration. *Z. Wasser Abwass. Forsch.* **12**, 73–83.
Sung W. and Morgan J. J. (1980) Kinetics and product of ferrous iron oxygenation in aqueous systems. *Environ. Sci. Technol.* **14**, 561–568.
Tamura H., Goto K. and Nagayama M. (1976) Effect of anions on the oxygenation of ferrous ion in neutral solutions. *J. Inorg. Nucl. Chem.* **38**, 113–117.
Tessenow U. (1974) Solution diffusion and sorption in the upper layers of lake sediments. IV. Reaction mechanisms and equilibria in the system iron-manganese-phosphate with regard to the accumulation of vivianite in Lake Ursee (In German with English summary). *Arch. Hydrobiol. Suppl.*, 1–79.
van der Grift B., Rozemeijer J. C., Griffioen J. and van der Velde Y. (2014) Iron oxidation kinetics and phosphate immobilization along the flow-path from groundwater into surface water. *Hydrol. Earth Syst. Sci.* **18**, 4687–4702.
Van der Velde Y., Rozemeijer J. C., de Rooij G. H., van Geer F. C. and Broers H. P. (2010) Field-scale measurements for separation of catchment discharge into flow route contributions. *Vadose Zone J.* **9**, 25–35.
Van Duijvenbooden W., Taat J. and Gast L. F. L. (1985) *National Goundwater Quality Monitoring Network: Final Report of the Implementation (in Dutch)*. National Institute for Public Health and the Environment, Leidschendam, The Netherlands, p. 129.
van Riemsdijk W. H., van der Linden A. M. A. and Boumans L. J. M. (1984) Phosphate sorption by soils: III. the P diffusion-precipitation model tested for three acid sandy soils. *Soil Sci. Soc. Am. J.* **48**, 545–548.
Vanlierde E., De Schutter J., Jacobs P. and Mostaert F. (2007) Estimating and modeling the annual contribution of authigenic sediment to the total suspended sediment load in the Kleine Nete Basin, Belgium. *Sed. Geol.* **202**, 317–332.
Viollier E., Inglett P. W., Hunter K., Roychoudhury A. N. and Van Cappellen P. (2000) The ferrozine method revisited: Fe(II)/Fe(III) determination in natural waters. *Appl. Geochem.* **15**, 785–790.
Voegelin A., Kaegi R., Frommer J., Vantelon D. and Hug S. J. (2010) Effect of phosphate, silicate, and Ca on Fe(III)-precipitates formed in aerated Fe(II)- and As(III)-containing water studied by X-ray absorption spectroscopy. *Geochim. Cosmochim. Acta* **74**, 164–186.
Voegelin A., Senn A. C., Kaegi R., Hug S. J. and Mangold S. (2013) Dynamic Fe-precipitate formation induced by Fe(II) oxidation in aerated phosphate-containing water. *Geochim. Cosmochim. Acta* **117**, 216–231.
Vollrath S., Behrends T. and van Cappellen P. (2012) Oxygen dependency of neutrophilic Fe(II) oxidation by leptothrix differs from abiotic reaction. *Geomicrobiol. J.* **29**, 550–560.
Wolthoorn A., Temminghoff E. J. M., Weng L. and van Riemsdijk W. H. (2004) Colloid formation in groundwater: effect of phosphate, manganese, silicate and dissolved organic matter on the dynamic heterogeneous oxidation of ferrous iron. *Appl. Geochem.* **19**, 611–622.

*Associate editor:* Christophe Tournassat